

Three-dimensional non-Bosonic non-Fermionic quasiparticle through a quantized topological defect of crystal dislocation

Mingda Li¹, Qichen Song¹, M. S. Dresselhaus² and Gang Chen¹

¹*Department of Mechanical Engineering, MIT, Cambridge, MA 02139, USA*

²*Department of Physics and Department of Electrical Engineering and Computer Sciences, MIT, Cambridge, MA 02139, USA*

It is a fundamental postulate that quasiparticles in 3D space obey either Bosonic or Fermionic statistics, satisfying either canonical commutation or anti-commutation relation¹. However, under certain constraints, such as the 2D dimensional constraint, canonical quantization algebra is allowed to break down², and quasiparticles can obey other statistics, such as anyonic statistics³. In this study, we show that dislons– the quasiparticles in 3D due to quantized displacement field of a dislocation– can also obey neither Bosonic nor Fermionic statistics due to the topological constraint of the dislocation. With this theory, an effective electron field theory based on the electron-dislon interaction is obtained, which consists of two types of interactions. One classical-type of interaction is reducible to the well-known deformation potential scattering, and the other quantum-type of interaction indicates an effective attraction between electrons. The role of dislocations in superconductivity is clarified as the competition between the classical and quantum interactions, showing excellent agreement with experiments.

Quasiparticles are fundamental emergent phenomena and building blocks in condensed matter physics, where a strongly-interacting microscopic system behaves like a weakly-interacting renormalized system⁴. In three-dimensional (3D) space, quasiparticles can be categorized as either Bosons or Fermions with canonical formalism, where Bosonic quasiparticles (aka collective excitations) include phonons, magnons, excitons, plasmons, etc., and Fermionic quasiparticles include quasi-electrons, holes and polarons, etc¹. The renaissance of new quasiparticle families, such as Weyl and Dirac semimetals^{5, 6, 7}, hourglass fermions⁸ and nodal-chain metals⁹, attract wide recent interest, yet the resulting excitations can still be characterized as fermions¹⁰ (or Bosons). On the other hand, in fact, when a constraint exists, the canonical formalism can break down if the constraint is inconsistent with the canonical commutation relations². For instance in particle physics, canonical quantization of quantum electrodynamics is inconsistent with the Coulomb Gauge condition¹¹, while in condensed matter

physics, lowering the dimension as a spatial constraint forbids the free exchange of particles, resulting in a nontrivial phase factor when one particle circulates around the other, namely anyonic statistics³.

In this study, we show that even the simplest 3D isotropic solid can also accommodate quasiparticles with neither purely Bosonic nor Fermionic behavior, due to the topological definition of a crystal dislocation $\oint_C d\mathbf{u} = -\mathbf{b}$, where \mathbf{u} is the lattice displacement field vector, \mathbf{b} is Burgers vector and C is an arbitrary loop enclosing the dislocation line¹². The resulting quasiparticle, “dislon”, upon quantizing the displacement field \mathbf{u} , is shown to be composed of two half-Bosonic fields. This can be understood intuitively through a comparison with a Dirac monopole, which also has to be characterized by two fields (but two classical vector fields) due to its nontrivial topology (Figure 1a)¹³. To explore the significance of this quasiparticle, the electron-dislocation interaction is studied in the present work, where the electron effective Hamiltonian is obtained using a method inspired by the Faddeev-Popov gauge fixing approach^{14, 15} to impose the dislocation’s topological constraint. The effective electron Hamiltonian is shown to be composed of three terms- a diagonal quadratic term (non-interacting electron), an off-diagonal quadratic term (classical scattering) and a quartic term (quantum-mechanical interaction). The classical scattering term describes the electron-dislocation scattering process with electron momentum transfer perpendicular to dislocation direction, which can be reduced to the well-known deformation potential scattering under long wavelength limit. On the other hand, the quantum interaction describes an effective attraction between electron pairs mediated by a quantized dislocation (Figure 1b). The elusive role of the crystal dislocation on superconductivity is clarified using this approach, where a modified BCS gap equation incorporating both the classical and quantum interactions is derived, capable of quantitatively describing the influence of the dislocation on the superconducting transition temperature T_c . It turns out that the competition between the classical and quantum interactions plays the governing role in determining T_c . To validate the theory, the T_c of as many as ten dislocated superconductors are compared and excellent agreement is obtained.

The foundation of the quantized dislocation

The best way to understand the quantized dislocation is probably to compare it with a phonon. A phonon is a quantized lattice wave which can be mode-expanded in terms of plane waves¹⁶:

$$\mathbf{u}^{ph}(\mathbf{R}) = \frac{1}{\sqrt{N}} \sum_{\mathbf{k}} u_{\mathbf{k}}^{ph} \boldsymbol{\epsilon}_{\mathbf{k}\lambda} e^{i\mathbf{k}\cdot\mathbf{R}} \quad (1)$$

where \mathbf{u}^{ph} is the lattice displacement at spatial position \mathbf{R} , $\mathbf{\epsilon}_{\mathbf{k}\lambda}$ is the polarization vector and $u_{\mathbf{k}}^{ph}$ is the lattice displacement in the \mathbf{k} -component mode. In the static limit, there is no displacement, i.e. $u_{\mathbf{k}}^{ph} = 0$. As to dislocation, inspired by mode-expansion work in 1D^{17, 18}, here we expand the lattice displacement for a dislocation line as

$$\mathbf{u}_i(\mathbf{R}) = \frac{1}{A} \sum_{\mathbf{k} \equiv (\mathbf{s}, \kappa)} F_i(\mathbf{k}) e^{i\mathbf{k} \cdot \mathbf{R}} u_{\mathbf{k}} \quad (2)$$

where A is the sample area, $u_{\mathbf{k}}$ is dimensionless displacement, $F_i(\mathbf{k})$ is an expansion function, \mathbf{s} denotes the 2D momentum perpendicular to the dislocation direction, and κ is the dislocation-direction momentum introduced here for later convenience. In a 3D isotropic solid, for a dislocation line along the z -direction and the glide plane within xz -plane, $F_i(\mathbf{k})$ can be written explicitly as

$$F_i(\mathbf{k}) \equiv F_i(\mathbf{s}; \kappa) = + \frac{1}{k_x k^2} \left(n_i (\mathbf{b} \cdot \mathbf{k}) + b_i (\mathbf{n} \cdot \mathbf{k}) - \frac{1}{(1-\nu)} \frac{k_i (\mathbf{n} \cdot \mathbf{k}) (\mathbf{b} \cdot \mathbf{k})}{k^2} \right) \quad (3)$$

where $i = x, y, z$ are the spatial components, \mathbf{n} is the glide plane normal direction, \mathbf{b} is the Burgers vector, and ν is the Poisson ratio. The reason for the mode expansion in Eq. (2) is straightforward. Under the following boundary condition,

$$\lim_{\kappa \rightarrow 0} u_{\mathbf{k}} \equiv \lim_{\kappa \rightarrow 0} u_{\mathbf{s}, \kappa} = 1, \text{ for } \forall \mathbf{s} \quad (4)$$

Eq. (2) becomes equivalent to textbook results of static dislocation, for both edge and screw dislocations (Supporting information I). In fact, Eq. (4) – the topological definition of the dislocation, i.e. the reducibility to a classical dislocation – can be considered as the essential starting point of this theory, leading to the breakdown of the canonical quantization.

A brief comparison of a phonon and a quantized dislocation (aka dislon) is summarized in Table 1.

The dislocation Hamiltonian in 3D

Using the mode expansion Eq. (2), the classical dislocation Hamiltonian composed of kinetic energy T and potential energy U can be written in the usual way¹⁹ as (Supporting information II)

$$H = T + U = \frac{\rho}{2} \int \sum_{i=1}^3 \dot{\mathbf{u}}_i^2(\mathbf{R}) d^3\mathbf{R} + \frac{1}{2} \int c_{ijkl} u_{ij} u_{kl} d^3\mathbf{R} = \frac{1}{2L} \sum_{\mathbf{k}} T(\mathbf{k}) \dot{u}_{\mathbf{k}} \dot{u}_{-\mathbf{k}} + \frac{1}{2L} \sum_{\mathbf{k}} U(\mathbf{k}) u_{\mathbf{k}} u_{-\mathbf{k}} \quad (5)$$

where ρ is the mass density, c_{ijkl} is the stiffness tensor which can be written as $c_{ijkl} = \lambda \delta_{ij} \delta_{kl} + \mu (\delta_{ik} \delta_{jl} + \delta_{il} \delta_{jk})$ with λ the Lamé's first parameter and μ the shear modulus in an isotropic medium, and the coefficients $T(\mathbf{k}) \equiv \rho |F(\mathbf{k})|^2$, $U(\mathbf{k}) \equiv (\lambda + \mu) [\mathbf{k} \cdot \mathbf{F}(\mathbf{k})]^2 + \mu k^2 |F(\mathbf{k})|^2$. By noticing that the conjugate momentum is defined as $p_{\mathbf{k}} = \frac{\partial L}{\partial \dot{u}_{\mathbf{k}}} = m_{\mathbf{k}} \dot{u}_{-\mathbf{k}}$, and by further defining $m_{\mathbf{k}} \equiv T(\mathbf{k})/L$, $\Omega_{\mathbf{k}} \equiv \sqrt{U(\mathbf{k})/T(\mathbf{k})}$, the classical dislocation Hamiltonian Eq. (5) can be rewritten in the following way

$$H = \sum_{\mathbf{k}} \frac{p_{\mathbf{k}} p_{-\mathbf{k}}}{2m_{\mathbf{k}}} + \sum_{\mathbf{k}} \frac{m_{\mathbf{k}} \Omega_{\mathbf{k}}^2}{2} u_{\mathbf{k}} u_{-\mathbf{k}} \quad (6)$$

This appears to be similar to the quantization of the phonon, but with a momentum-dependent mass term. However, there is huge difference due to the constraint Eq. (4). To see this, in order to obtain a quantized theory of Eq. (6), it is natural to introduce canonical quantization as the case of phonon

$$\begin{cases} u_{\mathbf{k}} = Z_{\mathbf{k}} [a_{\mathbf{k}} + a_{-\mathbf{k}}^+] \\ p_{\mathbf{k}} = \frac{i\hbar}{2Z_{\mathbf{k}}} [a_{\mathbf{k}}^+ - a_{-\mathbf{k}}] \end{cases} \quad (7)$$

where $Z_{\mathbf{k}} \equiv \sqrt{\hbar/2m_{\mathbf{k}}\Omega_{\mathbf{k}}}$ is a prefactor. However, if we adopt the usual Bosonic commutation relation $[a_{\mathbf{k}}, a_{\mathbf{k}'}^+] = \delta_{\mathbf{k}\mathbf{k}'}$, it can be shown that Bosonic commutator is incompatible with the boundary condition in Eq. (4):

$$\lim_{\kappa \rightarrow 0} \delta_{\mathbf{k}\mathbf{k}'} = \lim_{\kappa \rightarrow 0} [a_{\mathbf{s}, \kappa}, a_{\mathbf{s}, \kappa}^+] = \lim_{\kappa \rightarrow 0} \left[\frac{1}{Z_{\mathbf{k}}} - a_{-\mathbf{s}, -\kappa}^+, \frac{1}{Z_{\mathbf{k}}} - a_{-\mathbf{s}, -\kappa} \right] = -\lim_{\kappa \rightarrow 0} [a_{-\mathbf{s}, -\kappa}, a_{-\mathbf{s}, -\kappa}^+] = -\lim_{\kappa \rightarrow 0} \delta_{\mathbf{k}\mathbf{k}'}$$

which leads to a contradiction. Instead, we find that the following statistics is fully consistent with the boundary condition in Eq. (4):

$$[a_{\mathbf{k}}, a_{\mathbf{k}'}^+] = \delta_{\mathbf{k}\mathbf{k}'} \text{sgn}(\mathbf{k}) \quad (8)$$

where the vector-sgn function is defined based on a generalization of complex-sgn function as

$$\text{sgn}(\mathbf{k}) = \begin{cases} +1, & \text{if } k_x > 0 \\ -1, & \text{if } k_x < 0 \\ \text{sgn}(k_y, \kappa), & \text{if } k_x = 0 \end{cases}, \text{sgn}(k_y, \kappa) = \begin{cases} 1, & \text{if } k_y > 0 \\ -1, & \text{if } k_y < 0 \\ \text{sgn } \kappa, & \text{if } k_y = 0 \end{cases}, \text{sgn}(\kappa) = \begin{cases} 1, & \text{if } \kappa > 0 \\ -1, & \text{if } \kappa < 0 \\ 0, & \text{if } \kappa = 0 \end{cases} \quad (9)$$

The quasiparticle in Eq. (8) fully defines a quantized dislocation, which we call a “dislon”, while $\Omega_{\mathbf{k}}$ is understood as dislon dispersion. Now we have

$$\lim_{\kappa \rightarrow 0} \text{sgn}(\mathbf{k}) = \lim_{\kappa \rightarrow 0} [a_{s,\kappa}, a_{s,\kappa}^+] = \lim_{\kappa \rightarrow 0} \left[\frac{1}{Z_{\mathbf{k}}} - a_{-s,-\kappa}^+, \frac{1}{Z_{\mathbf{k}}} - a_{-s,-\kappa} \right] = -\lim_{\kappa \rightarrow 0} [a_{-s,-\kappa}, a_{-s,-\kappa}^+] = -\lim_{\kappa \rightarrow 0} \text{sgn}(-\mathbf{k}) = \lim_{\kappa \rightarrow 0} \text{sgn}(\mathbf{k})$$

showing perfect consistency between the constraint Eq. (4) and dislon algebra Eq. (8). A few useful identities relevant to Eq. (8) are listed in the Supporting Information II.

In other words, the topological constraint of the dislocation Eq. (4) prevents the quantized dislocation displacement from being purely Bosonic. In the following we prove that Eq. (8) actually indicates a Boson sea behavior composed to two half-Bosons. The concept of a Boson sea²⁰ is similar to a Fermi sea and has an origin from supersymmetry²¹: for fermions when wavevector k above the Fermi sea $k > k_F$, a normal electron creation operator $c_{k>k_F}^+$ is defined, while below the Fermi sea $k < k_F$, a hole creation operator is defined as $d_{k<k_F}^+ = c_{k<k_F}$. Here when \mathbf{k} is above the Boson sea $\text{sgn}(\mathbf{k}) > 0$, we have dislon creation operator $a_{\mathbf{k}>0}^+$, while when below Boson sea $\text{sgn}(\mathbf{k}) < 0$, we define a new operator $b_{-\mathbf{k}}^+ = a_{\mathbf{k}}$. In this way, we have $b_{-\mathbf{k}} = a_{\mathbf{k}}^+$ valid, and the operators $b_{\mathbf{k}}$ and $b_{\mathbf{k}}^+$ satisfies normal Bosonic algebra $[b_{\mathbf{k}}, b_{\mathbf{k}'}^+] = \delta_{\mathbf{k}\mathbf{k}'}$. The normal canonical quantization commutator is thereafter fully recovered

$$\begin{aligned} [a_{\mathbf{k}}, a_{\mathbf{k}'}^+] &= \delta_{\mathbf{k}\mathbf{k}'}, \text{ for } \text{sgn}(\mathbf{k}) > 0 \\ [b_{\mathbf{k}}, b_{\mathbf{k}'}^+] &= \delta_{\mathbf{k}\mathbf{k}'}, \text{ for } \text{sgn}(\mathbf{k}) < 0 \end{aligned} \quad (10)$$

The quantized dislocation Hamiltonian Eq. (6) can be written as (see Supporting information II)

$$H = \sum_{\mathbf{k}} \hbar \Omega(\mathbf{k}) a_{\mathbf{k}}^+ a_{\mathbf{k}} = \sum_{\mathbf{k} \geq 0} \hbar \Omega(\mathbf{k}) \left(a_{\mathbf{k}}^+ a_{\mathbf{k}} + \frac{1}{2} \right) + \sum_{\mathbf{k} \geq 0} \hbar \Omega(\mathbf{k}) \left(b_{\mathbf{k}}^+ b_{\mathbf{k}} + \frac{1}{2} \right) \quad (11)$$

where we have used the fact that $\Omega(\mathbf{k} = \mathbf{0}) = 0$, and the short-hand notation $\mathbf{k} \geq 0$ denoting $\text{sgn} \mathbf{k} \geq 0$.

The necessity of two Boson fields (Figure 1b) in representing a quantized dislocation resembles a Dirac monopole¹³, where two magnetic vector potentials have to be defined for the south and north poles, respectively (Figure 1a)- in both scenarios, due to the topological constraint, a single field quantity – whether a classical vector potential or a quantized Bosonic field – is simply not sufficient to describe the intrinsic topological feature.

The electron-dislon interaction

The generic electron-ion interacting Hamiltonian can be represented using the deformation potential approximation as¹⁶

$$H_{e-ion} = \int d^3\mathbf{R} \rho_e(\mathbf{R}) \sum_{j=1}^N \nabla_{\mathbf{R}} V_{ei}(\mathbf{R} - \mathbf{R}_j^0) \cdot \mathbf{u}_j \quad (12)$$

where $\rho_e(\mathbf{R})$ is the charge density operator which is defined as $\rho_e(\mathbf{R}) = en_e(\mathbf{R}) = \frac{e}{V} \sum_{\mathbf{k}\mathbf{p}\sigma} e^{-i\mathbf{p}\cdot\mathbf{R}} c_{\mathbf{k}+\mathbf{p}\sigma}^+ c_{\mathbf{k}\sigma}$,

the Coulomb potential $V_{ei}(\mathbf{R} - \mathbf{R}_j^0) = \frac{1}{V} \sum_{\mathbf{k}} V_{\mathbf{k}} e^{i\mathbf{k}\cdot(\mathbf{R}-\mathbf{R}_j^0)}$ has a Fourier component $V_{\mathbf{k}} \equiv \frac{4\pi Ze}{k^2 + k_{TF}^2}$, in which k_{TF} is the Thomas-Fermi screening wavenumber. Using Eq. (2), the electron-quantized dislocation (aka dislon) interacting Hamiltonian Eq. (12) can be further simplified as (see Supporting information III)

$$\begin{aligned} H_{e-dis} &= \sum_{\mathbf{k}\mathbf{k}\sigma} g_{\mathbf{k}} c_{\mathbf{k}'+\mathbf{k}\sigma}^+ c_{\mathbf{k}'\sigma} (a_{\mathbf{k}} + a_{-\mathbf{k}}^+) \\ &= \sum_{\substack{\mathbf{k}'\sigma \\ \mathbf{k} \geq 0}} g_{\mathbf{k}} c_{\mathbf{k}'+\mathbf{k}\sigma}^+ c_{\mathbf{k}'\sigma} (a_{\mathbf{k}} + b_{\mathbf{k}}) + \sum_{\substack{\mathbf{k}'\sigma \\ \mathbf{k} \geq 0}} g_{\mathbf{k}}^* c_{\mathbf{k}'-\mathbf{k}\sigma}^+ c_{\mathbf{k}'\sigma} (b_{\mathbf{k}}^+ + a_{\mathbf{k}}^+) \end{aligned} \quad (13)$$

with the electron-dislocation coupling constant $g_{\mathbf{k}} \equiv \frac{eN}{VA} V_{\mathbf{k}} [i\mathbf{k} \cdot \mathbf{F}(\mathbf{k})] \sqrt{\frac{\hbar}{2m_{\mathbf{k}}\Omega_{\mathbf{k}}}}$, and N is the number of ions in the system, and V is the sample volume. As a comparison, the electron-phonon interaction Hamiltonian is written as¹⁶

$$H_{e-ph} = \sum_{\mathbf{k}\mathbf{k}\sigma} g_{\mathbf{k}}^{ph} c_{\mathbf{k}'+\mathbf{k}\sigma}^+ c_{\mathbf{k}'\sigma} (A_{\mathbf{k}} + A_{-\mathbf{k}}^+) \quad (14)$$

with the electron-phonon coupling constant $g_{\mathbf{k}}^{ph} = \frac{ieV_{\mathbf{k}}}{V} (\mathbf{k} \cdot \boldsymbol{\varepsilon}_{\mathbf{k}}) \sqrt{\frac{N\hbar}{2M\omega_{\mathbf{k}}}}$. There are two major

differences between the electron-dislon interaction and the electron-phonon interaction

1. $a_{\mathbf{k}}$ for dislons are not purely Bosonic, but satisfy Eq. (8); for phonons, the operators $A_{\mathbf{k}}$ are Bosonic.
2. $g_{\mathbf{k}}$ and $g_{\mathbf{k}}^{ph}$ have different levels of extensivity, i.e. the dependence of scale L : $g_{\mathbf{k}}^{ph} \sim \frac{1}{L^{3/2}}$ while $g_{\mathbf{k}} \sim \frac{1}{L^2}$. This is quite reasonable since up to now we are studying a single dislocation only. For multiple independent dislocation, similar to the phonon case multiply \sqrt{N} where N is number of

ions, here, we multiply $g_{\mathbf{k}}$ by a factor of $\sqrt{N_D}$, where N_D is the number of dislocation. To do so, we recover the same scale dependence $g_{\mathbf{k}} \sim \frac{1}{L^{3/2}}$ as with a phonon. The factor of $\sqrt{N_D}$ is also necessary to correctly reproduce the classical relaxation rate (See below).

Therefore, for multiple independent dislocations, we have the electron-dislocation coupling constant

$$g_{\mathbf{k}} = \frac{eN}{VA} \sqrt{N_D} V_{\mathbf{k}} [i\mathbf{k} \cdot \mathbf{F}(\mathbf{k})] \sqrt{\frac{\hbar}{2m_{\mathbf{k}}\Omega_{\mathbf{k}}}} \quad (15)$$

Effective field theory of electrons

To see how electron-dislocation interaction Eq. (13) under the constraint of Eq. (4) really affects the material electronic properties, we adopt a functional integral approach²² to eliminate the dislon degree of freedom and establish an effective field theory for solely electrons. The total action of the interacting electron-dislon system can be written as

$$S_{tot}[\bar{\psi}, \psi, \bar{\chi}, \chi] = S_e[\bar{\psi}, \psi] + S_{dis}[\bar{\chi}_a, \chi_a, \bar{\chi}_b, \chi_b] + S_{e-dis}[\bar{\psi}, \psi, \bar{\chi}_a, \chi_a, \bar{\chi}_b, \chi_b] \quad (16)$$

where $\bar{\psi}, \psi$ are electron fields and $\bar{\chi}, \chi$ are dislon fields, with a and b are the 2 Bosonic components of a dislon. Now the non-interacting electron and dislon actions can be written as

$$\begin{aligned} S_e[\bar{\psi}, \psi] &= \sum_{n\mathbf{p}\sigma} \bar{\psi}_{n\mathbf{k}\sigma} (-ip_n + \varepsilon_{\mathbf{k}} - \mu) \psi_{n\mathbf{k}\sigma} \\ S_{dis}[\bar{\chi}, \chi] &= \sum_{n, \mathbf{k} \geq 0} [\bar{\chi}_{a\mathbf{k}n} (-i\omega_n + \hbar\Omega_{\mathbf{k}}) \chi_{a\mathbf{k}n} + \bar{\chi}_{b\mathbf{k}n} (-i\omega_n + \hbar\Omega_{\mathbf{k}}) \chi_{b\mathbf{k}n}] \end{aligned} \quad (17)$$

where $\omega_n \equiv 2n\pi T$, $p_n \equiv (2n+1)\pi T$ are Bosonic and Fermionic Matsubara frequencies, respectively.

The interaction Hamiltonian Eq. (13) can be also rewritten in action form as

$$S_{e-dis}[\bar{\psi}, \psi, \bar{\chi}, \chi] = \sum_{n, \mathbf{k} \geq 0} \frac{g_{\mathbf{k}}}{\sqrt{\beta}} \rho_{n\mathbf{k}} (\chi_{n\mathbf{k},a} + \chi_{n\mathbf{k},b}) + \sum_{n, \mathbf{k} \geq 0} \frac{g_{\mathbf{k}}^*}{\sqrt{\beta}} \rho_{-n-\mathbf{k}} (\bar{\chi}_{n\mathbf{k},a} + \bar{\chi}_{n\mathbf{k},b}) \quad (18)$$

where we have defined the charge density in momentum space as $\rho_{n\mathbf{k}} \equiv \sum_{\mathbf{k}'m\sigma} \bar{\psi}_{m+n, \mathbf{k}'+\mathbf{k}\sigma} \psi_{m\mathbf{k}'\sigma}$. To achieve

further simplification, we perform the Keldysh rotation²³, by defining that

$$\begin{aligned}
d_{\mathbf{k}n} &= \frac{1}{\sqrt{2}}(\chi_{\mathbf{k}n,a} + \chi_{\mathbf{k}n,b}), & \bar{d}_{\mathbf{k}n} &= \frac{1}{\sqrt{2}}(\bar{\chi}_{\mathbf{k}n,a} + \bar{\chi}_{\mathbf{k}n,b}) \\
f_{\mathbf{k}n} &= \frac{1}{\sqrt{2}}(-\chi_{\mathbf{k}n,a} + \chi_{\mathbf{k}n,b}), & \bar{f}_{\mathbf{k}n} &= \frac{1}{\sqrt{2}}(-\bar{\chi}_{\mathbf{k}n,a} + \bar{\chi}_{\mathbf{k}n,b})
\end{aligned} \tag{19}$$

Then the non-interacting dislon action in Eq. (17) and interaction action Eq. (18) can be rewritten as

$$\begin{aligned}
S_{dis} &= \sum_{n,\mathbf{k} \geq 0} \bar{d}_{\mathbf{k}n}(-i\omega_n + \hbar\Omega_{\mathbf{k}})d_{\mathbf{k}n} + \sum_{n,\mathbf{k} \geq 0} \bar{f}_{\mathbf{k}n}(-i\omega_n + \hbar\Omega_{\mathbf{k}})f_{\mathbf{k}n} \\
S_{e-dis}[\bar{\psi}, \psi, \bar{d}, d] &= \sum_{n,\mathbf{k} \geq 0} \sqrt{\frac{2}{\beta}} g_{\mathbf{k}} \rho_{n\mathbf{k}} d_{n\mathbf{k}} + \sum_{n,\mathbf{k} \geq 0} \sqrt{\frac{2}{\beta}} g_{\mathbf{k}}^* \rho_{-n-\mathbf{k}} \bar{d}_{n\mathbf{k}}
\end{aligned} \tag{20}$$

respectively. Now since the $f_{\mathbf{k}n}$ field from Eq. (20) is completely decoupled from the electron degree of freedom, it can be neglected when defining the electron effective action. The constraint in Eq. (4) can now be rewritten as

$$\begin{aligned}
\lim_{\kappa \rightarrow 0} d_{s,\kappa} &= d_{s0} = \lim_{\kappa \rightarrow 0} \sqrt{\frac{\beta m_{\mathbf{k}} \Omega_{\mathbf{k}}}{\hbar}} \equiv C_s \\
\lim_{\kappa \rightarrow 0} \bar{d}_{s,\kappa} &= \bar{d}_{s0} = \lim_{\kappa \rightarrow 0} \sqrt{\frac{\beta m_{\mathbf{k}} \Omega_{\mathbf{k}}}{\hbar}} = C_s
\end{aligned} \tag{21}$$

where $C_s = \lim_{\kappa \rightarrow 0} \sqrt{\frac{\beta m_{\mathbf{k}} \Omega_{\mathbf{k}}}{\hbar}}$ is an \mathbf{s} -dependent constant satisfying $\text{sgn}(\mathbf{s}) \geq 0$ since the original single displacement u_{s0} is divided into d_{s0} and \bar{d}_{s0} . With Eq. (20) at hand, the effective electron action can be defined in analog to the Faddeev-Popov gauge fixing method¹⁵ to impose the constraint Eq. (21) using δ -functions as

$$\exp(-S_{eff}[\bar{\psi}, \psi]) \equiv \exp(-S_e[\bar{\psi}, \psi]) \times \int \frac{D[\bar{d}, d] \prod_{n\mathbf{s} \geq 0} \delta(d_{n\mathbf{s}0} - C_s) \delta(\bar{d}_{n\mathbf{s}0} - C_s)}{\exp(-S_{dis}[\bar{d}, d] - S_{e-dis}[\bar{\psi}, \psi, \bar{d}, d])} \tag{22}$$

After a few functional integration steps (Supporting Information IV), we obtain the effective electron action upon the electron-dislocation interaction

$$S_{eff}[\bar{\psi}, \psi] = S_e[\bar{\psi}, \psi] - \sum_{n\mathbf{k}|\kappa \neq 0} \frac{\hbar \Omega_{\mathbf{k}} g_{\mathbf{k}}^* g_{\mathbf{k}}}{\beta(\omega_n^2 + \hbar^2 \Omega_{\mathbf{k}}^2)} \rho_{-n-\mathbf{k}} \rho_{n\mathbf{k}} + \sum_{\mathbf{k}n\sigma} \sum_{m,s} \frac{C_s}{\sqrt{2\beta}} (g_s \bar{\psi}_{n+m\mathbf{k}+s\sigma} + g_s^* \bar{\psi}_{n-m\mathbf{k}-s\sigma}) \psi_{n\mathbf{k}\sigma} \tag{23}$$

Noticing that in real materials, dislocations can arise in many directions, and moreover since the $\kappa \neq 0$ constraint in Eq. (23) only contains a small volume of phase space (which is negligible in the thermodynamic limit), we can safely relax this constraint. Now if performing an analytical continuation

step back to the real frequency and picking-up the Cooper channel in the quartic term, the effective electron Hamiltonian is finally written as a sum of three contributions, the non-interacting electron H_0 , and classical scattering H_c and quantum interaction H_q ,

$$H_{eff} = H_0 + H_c + H_q$$

$$= \sum_{\mathbf{k}\sigma} (\varepsilon_{\mathbf{k}} - \mu) c_{\mathbf{k}\sigma}^\dagger c_{\mathbf{k}\sigma} + \sum_{\mathbf{k}\sigma} \sum_{\mathbf{s}} (A_s c_{\mathbf{k}+\mathbf{s}\sigma}^\dagger + A_s^* c_{\mathbf{k}-\mathbf{s}\sigma}^\dagger) c_{\mathbf{k}\sigma} + \sum_{\mathbf{q}\mathbf{k}\mathbf{k}'} V_{eff}(\mathbf{q}) c_{\mathbf{k}+\mathbf{q}\uparrow}^\dagger c_{-\mathbf{k}\downarrow}^\dagger c_{-\mathbf{k}'+\mathbf{q}\downarrow} c_{\mathbf{k}'\downarrow} \quad (24)$$

in which the classical electron-dislocation scattering (Figure 1b green straight line) amplitude A_s is defined as

$$A_s = \frac{eN}{2VA} \sqrt{N_{dis}} V_s [i\mathbf{s} \cdot \mathbf{F}(\mathbf{s})] = \frac{ieN}{2VL} \sqrt{n_{dis}} V_s \left(\frac{1-2\nu}{1-\nu} \right) \frac{(\mathbf{n} \cdot \mathbf{s})(\mathbf{b} \cdot \mathbf{s})}{k_x s^2} \quad (25)$$

where $s \equiv \sqrt{k_x^2 + k_y^2}$. The quantum-mechanical electron-electron attractive interaction mediated by the retarded dislon (Figure 1b wavy line) is written as

$$V_{eff}(\mathbf{q}) = -\frac{\hbar\Omega_q g_q^* g_q}{-\omega^2 + \hbar^2\Omega_q^2} \sim -\frac{g_q^* g_q}{\hbar\Omega_q} = -\left(\frac{N}{VA}\right)^2 N_{dis} \frac{(eV_q)^2}{2m_q\Omega_q^2} [\mathbf{q} \cdot \mathbf{F}(\mathbf{q})]^2 \quad (26)$$

The \sim approximation is valid since electrons near Fermi surface can have very small energy transfer ω .

Eqs. (24)- (26) are the main result of electron Hamiltonian, showing how dislocations will interact with electrons from a quantitative many-body viewpoint. Interestingly, the effective attractive interaction mediated by the dislon Eq. (26) shares some structural similarity with the interaction mediated by the phonon²⁴, which leads to phonon-mediated superconductivity. Here the interaction has a different coupling constant and the phonon dispersion ω_q is replaced by dislon dispersion Ω_q , as compared in Table 1.

Classical electron-dislocation scattering

Qualitatively, the classical scattering term H_c is quite intuitive in describing an electron scattering process $\mathbf{k} \rightarrow \mathbf{k} + \mathbf{s}$ and $\mathbf{k} \rightarrow \mathbf{k} - \mathbf{s}$, with momentum changes only happening perpendicular to the dislocation direction with amplitude A_s and A_s^* , respectively (Figure 1b). Quantitatively, for an edge dislocation $\mathbf{b} = (b \ 0 \ 0)$, $\mathbf{b} \cdot \mathbf{s} = bk_x$, $\mathbf{n} \cdot \mathbf{s} = s \sin \theta$, the Fourier transform of the scattering amplitude gives (Supporting information V)

$$A^{Edge}(\mathbf{r}) = \int A_s^{Edge} e^{i\mathbf{s}\cdot\mathbf{r}} \frac{d^2\mathbf{s}}{4\pi^2} = \frac{N}{VL} \frac{2\pi Ze^2}{k_{TF}^2} \times \frac{b}{2\pi} \left(\frac{1-2\nu}{1-\nu} \right) \frac{\sin\theta}{r} \propto \frac{b}{2\pi} \left(\frac{1-2\nu}{1-\nu} \right) \frac{\sin\theta}{r} \quad (27)$$

Aside from a proportionality constant, Eq. (27) is in perfect agreement with the classical dislocation deformation scattering potential²⁵, where $\delta V = -\frac{a_c b}{2\pi} \left(\frac{1-2\nu}{1-\nu} \right) \frac{\sin\theta}{r}$ with a_c is the conduction band deformation potential which is an empirical parameter and has a similar order of magnitude with the prefactor in Eq. (27). For a screw dislocation in an isotropic crystal, it is well-known that only purely shear strain exists, causing no dilation or compression of the unit cells hence leading to no deformation potential scattering²⁵. This is consistent with the result in Eq. (25), that for a screw dislocation $\mathbf{b} = (0 \ 0 \ b)$, we have $A_s^{Screw} = 0$.

The classical scattering term H_c , despite being quadratic, is full of off-diagonal elements which complicates the computation. To further simplify the classical scattering terms, from physical grounds in the following we consider elastic dislocation-electron scattering only, so that the relaxation rate $\Gamma_{\mathbf{k}}$ can be computed using Fermi's Golden rule as

$$\Gamma_{\mathbf{k}} \equiv \frac{\hbar}{2\tau_{\mathbf{k}}} = \frac{\pi}{2} \sum_{\mathbf{s}} \left| \langle \mathbf{k} + \mathbf{s} | \hat{A}_c | \mathbf{k} \rangle \right|^2 \delta(\varepsilon_{\mathbf{k}+\mathbf{s}} - \varepsilon_{\mathbf{k}}) \quad (28)$$

where the sum is over all final states which transfer in-plane momentum but maintaining elastic scattering, and \hat{A}_c is the classical scattering amplitude operator. The relaxation rate can thus be computed explicitly as (Supporting Information V)

$$\Gamma_{\mathbf{k}} \sim \frac{\pi m^*}{4\hbar^2 k^2 k_{TF}^4} \left(\frac{Ze^2 N}{V} \right)^2 n_{dis} b^2 \left(\frac{1-2\nu}{1-\nu} \right)^2 \quad (29)$$

where m^* is electron effective mass. With the relaxation rate at hand, the original quadratic Hamiltonian in Eq. (24) can be approximated by a non-Hermitian Hamiltonian²⁶ with complex eigenvalues as

$$\begin{aligned} H_0 + H_c &= \sum_{\mathbf{k}\sigma} (\varepsilon_{\mathbf{k}} - \mu) c_{\mathbf{k}\sigma}^\dagger c_{\mathbf{k}\sigma} + \sum_{\mathbf{k}\sigma} \sum_{\mathbf{s}} (A_s c_{\mathbf{k}+\mathbf{s}\sigma}^\dagger + A_s^* c_{\mathbf{k}-\mathbf{s}\sigma}^\dagger) c_{\mathbf{k}\sigma} \\ &\approx \sum_{\mathbf{k}} (E_{\mathbf{k}} - \mu' + i\Gamma_{\mathbf{k}}) c_{\mathbf{k}\uparrow}^\dagger c_{\mathbf{k}\uparrow} + \sum_{\mathbf{k}} (E_{\mathbf{k}} - \mu' - i\Gamma_{\mathbf{k}}) c_{\mathbf{k}\downarrow}^\dagger c_{\mathbf{k}\downarrow} \end{aligned} \quad (30)$$

The reason for this definition is to preserve time-reversal symmetry which the original Hamiltonian processes²⁶, that $T(H_0 + H_c)T^{-1} = H_0 + H_c$. Meanwhile, since electron-dislocation scattering is expected to increase the electron effective mass and decrease the energy¹⁸, with the same order as $\Gamma_{\mathbf{k}}$, for simplicity we assume $E_{\mathbf{k}} - \mu' \approx \varepsilon_{\mathbf{k}} - \Gamma_{\mathbf{k}} - \mu$ valid.

Electron-dislon BCS superconductivity

With simplified diagonal quadratic Hamiltonian Eq. (30), we are now ready to study the effect of dislocation on superconductivity at a quantitative level. Unlike the well-understood role of dislocation in affecting superconducting critical magnetic field H_c due to flux-pinning mechanism²⁷, the role of dislocation to superconducting transition temperature T_c remains elusive. For instance, in superconducting tantalum, the decrease of superconducting transition temperature T_c is correlated with the decrease of the electron mean free path, while equal decreases of the mean free path by dislocation has no effect on T_c ²⁸. Anderson proposed a mechanism²⁹ of anisotropy which is capable of increasing T_c , however for the particular case of the dislocation, no quantitative agreement has been achieved. Here, under the local-coupling limit³⁰ (i.e. $V_{eff}(\mathbf{q})$ has no \mathbf{q} -dependence), the electron Hamiltonian Eq. (24) can be written as

$$H_{eff} = \sum_{\mathbf{k}} \left[(E_{\mathbf{k}} - \mu' + i\Gamma_{\mathbf{k}}) c_{\mathbf{k}\uparrow}^+ c_{\mathbf{k}\uparrow} + (E_{\mathbf{k}} - \mu' - i\Gamma_{\mathbf{k}}) c_{\mathbf{k}\downarrow}^+ c_{\mathbf{k}\downarrow} \right] - \frac{g_{dis}}{V} \sum_{\mathbf{q}\mathbf{k}\mathbf{k}'} c_{\mathbf{k}+\mathbf{q}\uparrow}^+ c_{-\mathbf{k}\downarrow}^+ c_{-\mathbf{k}'+\mathbf{q}\downarrow} c_{\mathbf{k}'\uparrow} \quad (31)$$

where

$$g_{dis} = -\langle V_{eff}(\mathbf{q}) \rangle V = \left(\frac{1-2\nu}{1-\nu} \right)^2 b^2 \left(\frac{N}{V} \right)^2 n_{dis} L \left\langle \frac{(eV_{\mathbf{q}})^2 (\mathbf{n} \cdot \mathbf{q})^2 (\mathbf{b} \cdot \mathbf{q})^2}{2m_{\mathbf{q}} \Omega_{\mathbf{q}}^2 q_x^2 q^4 b^2} \right\rangle \quad (32)$$

Now if we add the contribution from the phonon-induced electron attraction contribution g_{ph} , Eq. (31) can be further simplified as (Supporting information VI)

$$H_{eff} = \sum_{\mathbf{k}} \left[(E_{\mathbf{k}} - \mu' + i\Gamma_{\mathbf{k}}) c_{\mathbf{k}\uparrow}^+ c_{\mathbf{k}\uparrow} + (E_{\mathbf{k}} - \mu' - i\Gamma_{\mathbf{k}}) c_{\mathbf{k}\downarrow}^+ c_{\mathbf{k}\downarrow} \right] - g_T \int d^3r c_{\uparrow}^+(\mathbf{r}) c_{\downarrow}^+(\mathbf{r}) c_{\downarrow}(\mathbf{r}) c_{\uparrow}(\mathbf{r}) \quad (33)$$

where we have defined $c_{\mathbf{k}}^+ = \frac{1}{\sqrt{V}} \int d^3r e^{i\mathbf{k} \cdot \mathbf{r}} c^+(\mathbf{r})$, the total coupling constant coming from both the phonon and the dislon gives $g_T = g_{ph} + g_{dis}$. To obtain the superconducting transition temperature with the contribution from both phonons and dislocations, we adopt an auxiliary field approach at a mean-field level³¹ (Supporting information VI), finally we obtain that

$$\frac{1}{g_{ph} + g_{dis}} = N(\mu) \int_0^{\omega_D} \frac{\tanh\left(\frac{\xi + \Gamma + i\Gamma}{2T_c}\right) + \tanh\left(\frac{\xi + \Gamma - i\Gamma}{2T_c}\right)}{2(\xi + \Gamma)} d\xi \quad (34)$$

where ω_D is the Debye frequency, $N(\mu)$ is the density of states at the Fermi level. Since we are interested in electrons near the Fermi level and $\omega_D \ll \mu$, i.e. the decay mainly exists near the Fermi level, we have assumed a constant decay constant

$$\Gamma \sim \Gamma_{k_F} = \frac{\pi m^*}{4\hbar^2 k_F^2 k_{TF}^4} \left(\frac{Ze^2 N}{V} \right)^2 n_{dis} b^2 \left(\frac{1-2\nu}{1-\nu} \right)^2 \quad (35)$$

which is also consistent with the classical result³² aside from a phenomenological constant. From Eq. (34), the competition between the classical scattering Γ and the quantum interaction g_{dis} is revealed (Figure 2). It can be seen clearly that if the quantum interaction dominates $g_{dis}/g_{ph} \gg \Gamma/\omega_D$, the superconducting transition temperature increases, and vice versa. In particular, the near-linearity of the $T_c = T_c^0$ curve (black-dotted line) indicates the possibility to use a single parameter, the quantum-to-classical ratio

$$\frac{Quantum}{Classical} \sim \frac{g_{dis}/g_{ph}}{\Gamma/\omega_D} \sim \frac{32\pi\hbar^2 k_F^2 \left(\frac{1-\nu}{1-2\nu} \right)^2}{m^* b^2 (\lambda + 2\mu) L} \frac{\omega_D}{g_{ph}} = \frac{32\pi\hbar^2 k_F^2 \left(\frac{1-\nu}{1-2\nu} \right)^2}{m^* b^2 (\lambda + 2\mu) L} \frac{\omega_D N(\mu)}{[N(\mu)g_{ph}]} \quad (36)$$

to estimate whether the dislocation will increase or decrease T_c . For easier comparison with experiments (Table 2), we note that g_{ph} has the usual energy unit hence Eq. (36) is dimensionless (Supporting information VII). For possible increase of T_c , it is preferable for a material to have a small effective mass m^* , lower values of rigidity λ and μ , and a smaller system size L . What is striking is that a combination of many generally-considered independent parameters appearing in Eq. (36), such as electronic properties and material properties, still gives a reasonably comparable quantity of coupling strength.

Experimental Comparison

Now we are ready to compare the theory using Eqs. (34) and (36) with experiments. In fact, the advantage of Eq. (36) is quite straightforward, since the dislocation density n_{dis} - which is required to compute the absolute magnitude of g_{dis} and Γ but is often missing due to the paucity of experimental data- is cancelled out (See Methods). We see that even at this level of approximation, the predicted T_c show excellent quantitative agreement with experiments (Table 2).

In addition to the small influences of dislocation on superconductivity, it is worth mentioning that in some semiconducting monochalcogenide superlattice structures^{33, 34} such as PbTe/PbS, introducing dislocations could drive a semiconductor-superconductor phase transition directly when the thin film thickness is small enough. Although some qualitative explanation of the pressure-induced phase transition or dislocation induced flat band³⁵ were given, no quantitative agreement has been reached to explain the origin of the superconductivity in these systems. Despite the scarcity of data compared with simple metals prevents a full calculation of magnitude of T_c in this system, given its very small effective mass³⁶, low rigidity³⁷ and small dislocation grid period, the estimated quantum-to-classical ratio according to Eq. (36) is expected to be exceedingly high, leading to a great enhancement of superconducting transition temperature.

Conclusions

In this study, we show that due to dislocation's topological constraint Eq. (4), a quantized dislocation has to obey a different commutation relation Eq. (8). The resulting new quasiparticle, the “dislon”, is the first example of 3D system showing behaviors beyond ordinary Bosonic and Fermionic statistics. As a result, the influence of dislocation on electrons is revealed to be composed of two distinct parts, a well-known classical scattering, and a new type of interaction which couples electron pairs through a dislon (Eqs. (24)-(26)). This theory may enable an investigation to enter into a no-man's land, to study the interplay between the crystal dislocation and other components of materials, such as electrons, phonons, magnetic moments, photons. Such studies would help to understand the role of dislocation on material electronic, thermal, magnetic and optical properties etc. at a new level of clarity.

Methods

Experimental Magnitudes

The simple metal material data are taken from the Landolt–Börnstein database³⁸ and a few others^{39, 40, 41} to ensure consistency, while the data for dislocated superconductors are taken separately^{42, 43, 44, 45, 46, 47}, which are all compiled in Table 2. Since the dislocation density is unknown for the majority of materials, while the ratio in Eq. (36) does not fix the absolute magnitude of g_{dis} , we have chosen a reasonably estimated value $g_{dis} = 0.02g_{ph}$ to scale all materials (take dislocation density $n_D \sim 10^{12} cm^{-2}$,

$L=10nm$ and other values from Zn as example, $\frac{g_{dis}}{g_{ph}} \sim \left(\frac{N}{V}\right)^2 \frac{n_{dis}}{L} \frac{(4\pi Ze^2)^2}{2k_{TF}^4 (\lambda + 2\mu)}$. A different choice of parameters in the reasonable range would slightly change the magnitude but not qualitative behavior. Since g_{dis} and Γ have different dimensions, for computational purpose we normalize $g_{dis} \rightarrow g_{dis}/V$ to match experimental dimensions of g_{dis} so as all coupling strength has energy dimension. For estimation of the Fermi-wavevector using the free-electron model, we use $k_F = \left(\frac{9\pi}{4}\right)^{1/3} \frac{1}{a_0 r_s}$, where the density parameter is defined as $\frac{4\pi}{3} n a_0^3 r_s^3 \equiv 1$.

References

1. Mahan GD. *Many-particle physics*, 3rd edn. Kluwer Academic/Plenum Publishers: New York, 2000.
2. Kleinert H. *Path integrals in quantum mechanics, statistics, polymer physics, and financial markets*, 5th edn. World Scientific: New Jersey, 2009.
3. Nayak C, Simon SH, Stern A, Freedman M, Das Sarma S. Non-Abelian anyons and topological quantum computation. *Rev Mod Phys* 2008, **80**(3): 1083-1159.
4. Anderson PW. *Concepts in solids : lectures on the theory of solids*. Addison-Wesley, Advanced Book Program: Redwood City, Calif., 1992.
5. Weng HM, Fang C, Fang Z, Bernevig BA, Dai X. Weyl Semimetal Phase in Noncentrosymmetric Transition-Metal Monophosphides. *Phys Rev X* 2015, **5**(1).
6. Huang SM, Xu SY, Belopolski I, Lee CC, Chang GQ, Wang BK, *et al.* A Weyl Fermion semimetal with surface Fermi arcs in the transition metal mononictide TaAs class. *Nat Commun* 2015, **6**.
7. Borisenko S, Gibson Q, Evtushinsky D, Zabolotnyy V, Büchner B, Cava RJ. Experimental Realization of a Three-Dimensional Dirac Semimetal. *Phys Rev Lett* 2014, **113**(2).
8. Wang ZJ, Alexandradinata A, Cava RJ, Bernevig BA. Hourglass fermions. *Nature* 2016, **532**(7598): 189-194.
9. Bzdušek T, Wu Q, Rüegg A, Sigrist M, Soluyanov AA. Nodal-chain metals. *Nature* 2016, advance online publication.
10. Bradlyn B, Cano J, Wang Z, Vergniory MG, Felser C, Cava RJ, *et al.* Beyond Dirac and Weyl fermions: Unconventional quasiparticles in conventional crystals. *Science* 2016, **353**(6299).
11. Weinberg S. *The quantum theory of fields*. Cambridge University Press: Cambridge ; New York, 1995.
12. Nabarro FRN. *Theory of crystal dislocations*. Dover Publications: New York, 1987.
13. Nakahara M. *Geometry, topology, and physics*, 2nd edn. Institute of Physics Publishing: Bristol ; Philadelphia, 2003.
14. Faddeev LD, Popov VN. Feynman diagrams for the Yang-Mills field. *Physics Letters B* 1967, **25**(1): 29-30.

15. Gribov VN. Quantization of Non-Abelian Gauge Theories. *Nucl Phys B* 1978, **139**(1-2): 1-19.
16. Bruus H, Flensberg K. *Many-body quantum theory in condensed matter physics : an introduction*. Oxford University Press: Oxford ; New York, 2004.
17. Li M, Ding Z, Meng Q, Zhou J, Zhu Y, Liu H, *et al.* The Non-Perturbative Quantum Nature of the Dislocation-Phonon Interaction. *ArXiv e-prints*; 2016.
18. Li M, Cui W, Dresselhaus MS, Chen G. Canonical Quantization of Crystal Dislocation and Electron-Dislocation Scattering in an Isotropic Medium. *ArXiv e-prints*; 2015.
19. Landau LD, Lifshits EM, Kosevich AdM, Pitaevskii LP. *Theory of elasticity*, 3rd English edn. Pergamon Press: Oxford Oxfordshire ; New York, 1986.
20. Nielsen HB, Ninomiya M. Dirac Sea for Bosons. *ArXiv High Energy Physics - Theory e-prints*; 1998.
21. Habara Y, Nielsen HB, Ninomiya M. Boson Sea Versus Dirac Sea. *International Journal of Modern Physics A* 2004, **19**: 5561-5583.
22. Negele JW, Orland H. *Quantum many-particle systems*. Addison-Wesley Pub. Co.: Redwood City, Calif., 1988.
23. Kamenev A. Many-body theory of non-equilibrium systems. *eprint arXiv:cond-mat/0412296*; 2004.
24. Aynajian P. *Electron-phonon interaction in conventional and unconventional superconductors*. Springer: Heidelberg ; New York, 2010.
25. Wood CEC, Jena D. *Polarization effects in semiconductors : from ab initio theory to device application*. Springer: New York, 2008.
26. Bender CM. Making sense of non-Hermitian Hamiltonians. *Rep Prog Phys* 2007, **70**(6): 947-1018.
27. Larkin AI, Ovchinnikov YN. Pinning in type II superconductors. *J Low Temp Phys* 1979, **34**(3): 409-428.
28. Seraphim DP, Novick DT, Budnick JI. The Effects of Imperfections on the Superconducting Critical Temperature of Tantalum. *Acta Metall Mater* 1961, **9**(5): 446-452.
29. Anderson PW. Theory of Dirty Superconductors. *J Phys Chem Solids* 1959, **11**(1-2): 26-30.
30. Schrieffer JR. *Theory of superconductivity*. Advanced Book Program, Perseus Books: Reading, Mass., 1999.
31. Nagaosa N. *Quantum field theory in condensed matter physics*. Springer: Berlin ; New York, 1999.
32. Dexter DL, Seitz F. Effects of Dislocations on Mobilities in Semiconductors. *Phys Rev* 1952, **86**(6): 964-965.
33. Fogel NY, Buchstab EI, Bomze YV, Yuzepovich OI, Sipatov AY, Pashitskii EA, *et al.* Interfacial superconductivity in semiconducting monochalcogenide superlattices. *Physical Review B* 2002, **66**(17): 174513.
34. Fogel NY, Pokhila AS, Bomze YV, Sipatov AY, Fedorenko AI, Shekhter RI. Novel Superconducting Semiconducting Superlattices: Dislocation-Induced Superconductivity? *Physical Review Letters* 2001, **86**(3): 512-515.
35. Tang E, Fu L. Strain-induced partially flat band, helical snake states and interface superconductivity in topological crystalline insulators. *Nat Phys* 2014, **10**(12): 964-969.
36. Lead telluride (PbTe) effective masses. In: Madelung O, Rössler U, Schulz M (eds). *Non-Tetrahedrally Bonded Elements and Binary Compounds I*. Springer Berlin Heidelberg: Berlin, Heidelberg, 1998, pp 1-3.

37. Ni JE, Case ED, Khabir KN, Stewart RC, Wu CI, Hogan TP, *et al.* Room temperature Young's modulus, shear modulus, Poisson's ratio and hardness of PbTe-PbS thermoelectric materials. *Mater Sci Eng B-Adv* 2010, **170**(1-3): 58-66.
38. The Landolt-Börnstein Database. In: Villars P, editor.: Springer-Verlag Berlin Heidelberg & Material Phases Data System (MPDS); 2014.
39. Morel P, Anderson PW. Calculation of the Superconducting State Parameters with Retarded Electron-Phonon Interaction. *Phys Rev* 1962, **125**(4): 1263-1271.
40. Visscher PB, Falicov LM. Fermi-Surface Properties of Metals. *Phys Status Solidi B* 1972, **54**(1): 9-51.
41. Rose JH, Shore HB. Uniform electron gas for transition metals: Input parameters. *Physical Review B* 1993, **48**(24): 18254-18256.
42. Joiner WCH. Effects of Dislocations on the Superconducting Transition Temperature of Aluminum and Aluminum Alloys. *Phys Rev* 1965, **137**(1A): A112-A118.
43. Steele MC, Hein RA. Superconductivity of Titanium. *Phys Rev* 1953, **91**(2): 490-490.
44. von Minnigerode G. Der Einfluß von Gitterfehlern auf die Übergangstemperaturen verschiedener Supraleiter. *Zeitschrift für Physik* 1959, **154**(4): 442-459.
45. Schenck JF, Shaw RW. Plastic Deformation and Superconductivity in Lead, Indium, and Thallium. *J Appl Phys* 1969, **40**(13): 5165-&.
46. Krah W, Kohnlein D. Influence of Plastic-Deformation on Superconductivity of Vanadium and Niobium. *Z Phys B Con Mat* 1977, **28**(1): 19-22.
47. Köhnlein D. Supraleitung von Vanadium, Niob und Tantal unter hohem Druck. *Zeitschrift für Physik* 1968, **208**(2): 142-158.

Acknowledgements

ML would thank H. Liu, R. Jaffe, O. Yuzepovich, J. Synder, L. Fu, L. Meroueh and R. Hanus for their helpful discussions. ML, QS, MSD and GC would like to thank support by S³TEC, an Energy Frontier Research Center funded by U.S. Department of Energy (DOE), Office of Basic Energy Sciences (BES) under Award No. DE-SC0001299/DE-FG02-09ER46577.

Additional information

Supplementary information is available in the online version of the paper. Reprints and permissions information is available online. Correspondence and requests for materials should be addressed to ML (mingda@mit.edu) or GC (gchen2@mit.edu).

Competing financial interests

The authors declare no competing financial interests.

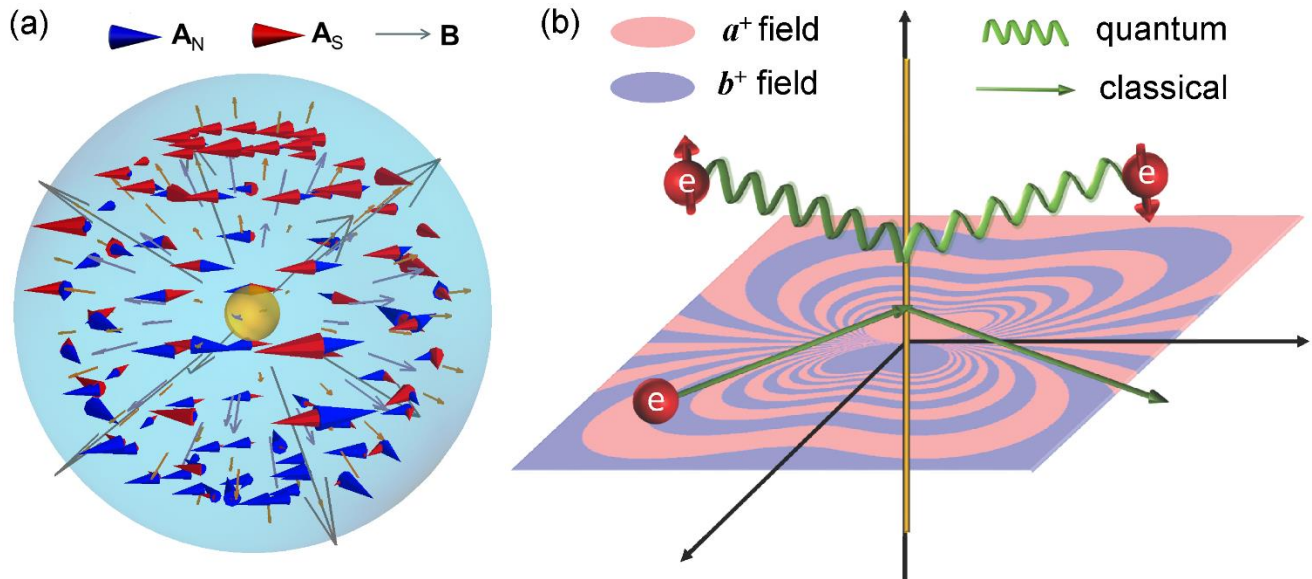


Figure 1 | Dirac monopole vs Quantized dislocation. In (a), to describe a Dirac monopole (golden sphere), two classical magnetic vector potentials (A_N and A_S) have to be implemented due to the non-trivial topology, giving the same magnetic field B (arrows). In (b), to describe a quantized dislocation (golden line), two quantum fields (a^+ and b^+) are implemented to capture the topology. The color of the field distribution is for illustrative purpose only. The electron-dislocation interactions have two types. The classical interaction (green straight lines with arrows) denotes the momentum-transfer scattering resulting in weakened superconductivity, while another quantum interaction (green wavy lines) leads to an effective attraction between electrons, resulting in enhanced superconductivity.

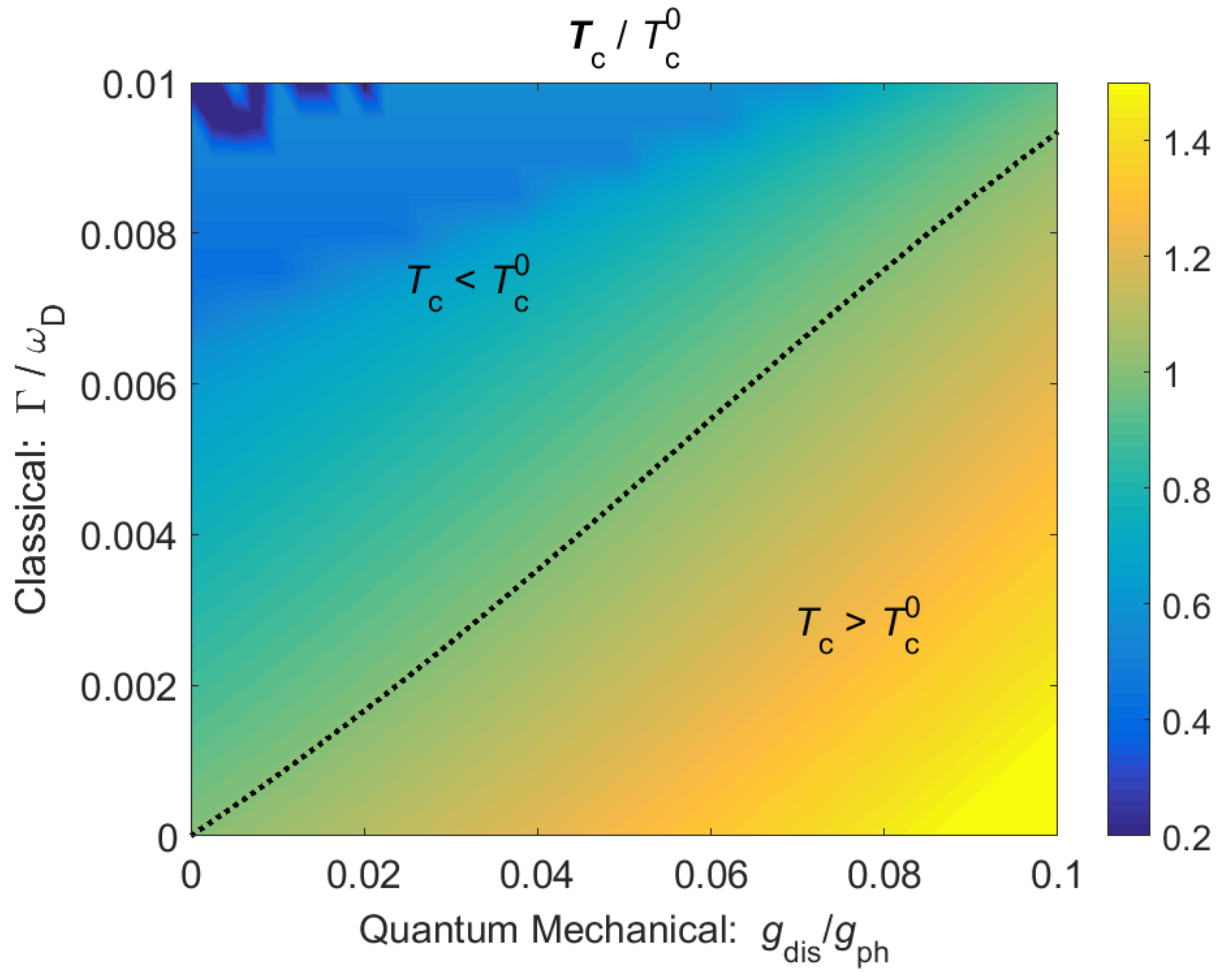


Figure 2 | Competition between classical and quantum interactions. There is a clear line (black-dotted) separating the dislocation-enhanced superconductivity ($T_c > T_c^0$) region from dislocation-weakened superconductivity ($T_c < T_c^0$) region.

Table 1 | Comparison between a phonon and a dislon. The topological constraint of a dislocation leads to a series of differences compared with a phonon, but still sharing many structural similarities.

	Phonon	Quantized dislocation (Dislon)
Essence	small displacement \mathbf{u}	displacement \mathbf{u} with constraint $\oint d\mathbf{u} = -\mathbf{b}$
Mode expansion	$\mathbf{u}(\mathbf{R}) \sim \sum_{\mathbf{k}} u_{\mathbf{k}} \boldsymbol{\varepsilon}_{\mathbf{k}} e^{i\mathbf{k} \cdot \mathbf{R}}$	$\mathbf{u}(\mathbf{R}) \sim \sum_{\mathbf{k}} u_{\mathbf{k}} \mathbf{F}(\mathbf{k}) e^{i\mathbf{k} \cdot \mathbf{R}}$
Static limit	$\lim_{\kappa \rightarrow 0} u_{\mathbf{k}} = 0$	$\lim_{\kappa \rightarrow 0} u_{\mathbf{k}} = 1$
Electron-interaction	$H_{e-ph} = \sum_{\mathbf{k}\mathbf{k}\sigma} g_{\mathbf{k}}^{ph} c_{\mathbf{k}'+\mathbf{k}\sigma}^{\dagger} c_{\mathbf{k}'\sigma} (A_{\mathbf{k}} + A_{-\mathbf{k}}^{\dagger})$	$H_{e-dis} = \sum_{\mathbf{k}\mathbf{k}\sigma} g_{\mathbf{k}} c_{\mathbf{k}'+\mathbf{k}\sigma}^{\dagger} c_{\mathbf{k}'\sigma} (a_{\mathbf{k}} + a_{-\mathbf{k}}^{\dagger})$
Algebra	Bosonic $[A_{\mathbf{k}}, A_{\mathbf{k}'}^{\dagger}] = \delta_{\mathbf{k}\mathbf{k}'}$	Two half-Bosons $[a_{\mathbf{k}}, a_{\mathbf{k}'}^{\dagger}] = \delta_{\mathbf{k}\mathbf{k}'} \text{sgn}(\mathbf{k})$
Coupling Constant with electron	$g_{\mathbf{k}}^{ph} = \frac{ieV_{\mathbf{k}}}{V} (\mathbf{k} \cdot \boldsymbol{\varepsilon}_{\mathbf{k}}) \sqrt{\frac{\hbar N}{2M\omega_{\mathbf{k}}}}$	$g_{\mathbf{k}} \equiv \frac{ieN}{VA} V_{\mathbf{k}} [\mathbf{k} \cdot \mathbf{F}(\mathbf{k})] \sqrt{\frac{\hbar N_D}{2m_{\mathbf{k}}\Omega_{\mathbf{k}}}}$
Effective Electron-electron interaction	$V_{eff}^{ph}(\mathbf{q}) = -\frac{\hbar\omega_{\mathbf{q}} g_{\mathbf{q}}^{ph} ^2}{-\omega^2 + \hbar^2\omega_{\mathbf{q}}^2}$	$V_{eff}(\mathbf{q}) = -\frac{\hbar\Omega_{\mathbf{q}} g_{\mathbf{q}}^* g_{\mathbf{q}}}{-\omega^2 + \hbar^2\Omega_{\mathbf{q}}^2}$
Superconductivity	$\frac{1}{g_{ph}} = N(\mu) \int_0^{\omega_D} \frac{\tanh\left(\frac{\lambda(\xi)}{2T}\right)}{\lambda(\xi)} d\xi$	$\frac{1}{g_{\tau}} = N(\mu') \int_0^{\omega_D} \frac{\sum_{s=\pm 1} \tanh\left(\frac{\lambda(\xi) + is\Gamma}{2T}\right)}{2\lambda(\xi)} d\xi$

Table 2 | Comparison between theory and experimental data of superconducting transition temperature for a series of simple-metal dislocated superconductors. With input of material electronic properties parameters such as the density of state at Fermi level ($N(\mu)$), the electron effective mass m^* and the Fermi wavevector k_F etc., and material mechanical properties including the Poisson ratio ν , the shear modulus μ , the superconducting transition temperature with the presence of dislocation T_c can be computed and compared with experimental value $[T_c]_{\text{exp}}$. The theory gives a correct trend of all materials.

	Al	In	Nb	Pb	Sn	Ta	Ti	Tl	V	Zn
Type	I	I	II	I	I	I	I	I	II	I
$N(\mu)g_{ph}$	0.175	0.29	0.29	0.36	0.245	0.25	0.15	0.27	0.24	0.165
$N(\mu)$ (eV ⁻¹)	0.41	0.334	0.87	0.26	0.05	0.76	0.463	0.73	1.01	0.314
ω_D (K)	433	112	276	105	199	246	420	78.5	399	329
$[T_c^0]_{\text{exp}}$ (K)	1.2	3.37	9.42	7.21	3.72	4.46	0.49	2.2	5.47	0.9
$[T_c]_{\text{exp}}$ (K)	1.2	3.51	9.94	7.21	3.95	4.46	0.37	2.48	5.94	1.39
k_F (nm ⁻¹)	17.5	15.0	18.9	15.7	16.2	19.5	17.5	13.5	19.5	15.7
m^*/m_e	1.10	0.11	0.53	1.58	0.035	0.82	1.43	0.87	1.30	1.25
μ (GPa)	26	4	38	5.6	18	69	44.0	2.8	47	43
λ (GPa)	59	32	145	42	46	154	81	41	129	41
ν	0.35	0.45	0.40	0.44	0.36	0.34	0.32	0.45	0.37	0.25
Q/CV	14.0	234	26.7	5.68	22.8	5.93	6.88	33.9	15.2	2.57

$\left[T_c/T_c^0\right]_{\text{Exp}}$	1.00	1.04	1.06	1.00	1.06	1.00	0.75	1.13	1.09	1.54
$\left[T_c/T_c^0\right]_{\text{Theory}}$	0.94	1.07	1.06	1.03	1.06	1.01	0.87	1.07	1.05	1.28
Experiment Trend	—	↑	↑	—	↑	—	↓	↑	↑	↑
Predicted Trend	↓	↑	↑	↑	↑	—	↓	↑	↑	↑

Supporting information of “*Three-dimensional non-Bosonic non-Fermionic quasiparticle through a quantized topological defect of crystal dislocation*”

Mingda Li¹, Qichen Song¹, M. S. Dresselhaus² and Gang Chen¹

¹*Department of Mechanical Engineering, MIT, Cambridge, MA 02139, USA*

²*Department of Physics and Department of Electrical Engineering and Computer Sciences, MIT, Cambridge, MA 02139, USA*

Correspondence to: mingda@mit.edu (ML) and gchen2@mit.edu (GC)

I. The classical static limit

We explicitly compute Eq. (2) in the main text to see why Eq. (4) ensure the displacement of a dislocation. For a screw dislocation along the z-direction, we have $\mathbf{b} = (0 \ 0 \ b)$ and $n = (0 \ 1 \ 0)$, hence in the classical limit $\kappa \rightarrow 0$, we have

$F_x(\mathbf{s}) = 0$, $F_y(\mathbf{s}) = 0$, and $F_z(\mathbf{s}) = \frac{b}{s^2} \frac{k_y}{k_x}$. This gives a displacement $\mathbf{u}_x(\mathbf{R}) = \mathbf{u}_y(\mathbf{R}) = 0$, and most importantly, $\mathbf{u}_z(\mathbf{R}) = \frac{1}{A} \sum_{\mathbf{s}} e^{i\mathbf{s} \cdot \mathbf{r}} \times \frac{1}{s^2} \frac{bk_y}{k_x} = \frac{b}{4\pi^2} \int \frac{k_y}{k_x(k_x^2 + k_y^2)} e^{ixk_x + iyk_y} dk_x dk_y = \frac{b}{2\pi} \arctan\left(\frac{y}{x}\right)$, which is identical with the well-known classical results¹.

For an edge dislocation, we have $\mathbf{b} = (b \ 0 \ 0)$, $n = (0 \ 1 \ 0)$, giving $F_z(\mathbf{s}) = 0$

$F_x(\mathbf{s}) = + \frac{b}{k_x s^2} \left(k_y - \frac{1}{(1-\nu)} \frac{k_x^2 k_y}{s^2} \right)$ and $F_y(\mathbf{s}) = + \frac{b}{k_x s^2} \left(k_x + \frac{1}{(1-\nu)} \frac{k_y^2 k_x}{s^2} \right)$. The corresponding displacements are $\mathbf{u}_z(\mathbf{R}) = 0$,

$$\mathbf{u}_x(\mathbf{R}) = \frac{b}{4\pi^2} \int dk_x dk_y \frac{e^{ik_x x + ik_y y}}{k_x^2 + k_y^2} \left(\frac{k_y}{k_x} - \frac{1}{(1-\nu)} \frac{k_x k_y}{k_x^2 + k_y^2} \right) = \frac{b}{2\pi} \left[\tan^{-1}\left(\frac{y}{x}\right) + \frac{1}{2(1-\nu)} \frac{xy}{x^2 + y^2} \right]$$

$$\mathbf{u}_y(\mathbf{R}) = \frac{b}{4\pi^2} \int dk_x dk_y \frac{e^{ik_x x + ik_y y}}{k_x^2 + k_y^2} \left(1 - \frac{1}{(1-\nu)} \frac{k_y^2}{k_x^2 + k_y^2} \right) = -\frac{b}{2\pi} \left[\frac{1-2\nu}{2(1-\nu)} \ln \sqrt{x^2 + y^2} + \frac{1}{2(1-\nu)} \frac{x^2}{x^2 + y^2} \right]$$

which all nicely reduced to well-known classical results. In other words, the full definition of the dislocation $\oint d\mathbf{u} = -\mathbf{b}$ is greatly reduced to an equivalent but much simpler condition of Eq. (4) in the main text.

II. Hamiltonian of the crystal dislocation in its 3D form

The total kinetic energy can be written as

$$\begin{aligned} T &= \frac{\rho}{2} \int \sum_{i=1}^3 \dot{\mathbf{u}}_i^2(\mathbf{R}) d^3\mathbf{R} = \frac{\rho}{2A^2} \int \sum_{i=1}^3 \sum_{\mathbf{k}\mathbf{k}'} F_i(\mathbf{k}) F_i(\mathbf{k}') e^{i(\mathbf{k}+\mathbf{k}')\cdot\mathbf{R}} \dot{u}_{\mathbf{k}} \dot{u}_{\mathbf{k}'} d^3\mathbf{R} \\ &= \frac{\rho}{2L} \sum_{i=1}^3 \sum_{\mathbf{k}} F_i(\mathbf{k}) F_i(-\mathbf{k}) \dot{u}_{\mathbf{k}} \dot{u}_{-\mathbf{k}} = \frac{\rho}{2L} \sum_{\mathbf{k}} |F(\mathbf{k})|^2 \dot{u}_{\mathbf{k}} \dot{u}_{-\mathbf{k}} \end{aligned} \quad (\text{II.1})$$

Since the distortion tensor can be computed based as

$$u_{ij}(\mathbf{R}) = u_{ji}(\mathbf{R}) = \frac{1}{2} \left(\frac{\partial \mathbf{u}_i}{\partial R_j} + \frac{\partial \mathbf{u}_j}{\partial R_i} \right) = \frac{1}{A} \sum_{\mathbf{k}=(\mathbf{s},\kappa)} i \frac{k_j F_i(\mathbf{k}) + k_i F_j(\mathbf{k})}{2} e^{i\mathbf{k}\cdot\mathbf{R}} u_{\mathbf{k}} \quad (\text{II.2})$$

The total potential can be written as

$$\begin{aligned} U &= \frac{1}{2} \int c_{ijkl} u_{ij} u_{kl} d^3\mathbf{R} = \frac{1}{2} \int (\lambda u_{ii} u_{kk} + \mu (u_{ij} u_{ij} + u_{ij} u_{ji})) d^3\mathbf{R} \\ &= -\frac{\lambda}{2} \int \frac{1}{A^2} \sum_{\mathbf{k},\mathbf{k}'} [\mathbf{k} \cdot \mathbf{F}(\mathbf{k})] [\mathbf{k}' \cdot \mathbf{F}(\mathbf{k}')] e^{i(\mathbf{k}+\mathbf{k}')\cdot\mathbf{R}} u_{\mathbf{k}} u_{\mathbf{k}'} d^3\mathbf{R} \\ &\quad - \frac{\mu}{A^2} \int \sum_{\mathbf{k},\mathbf{k}',i,j} \frac{[k_j F_i(\mathbf{k}) + k_i F_j(\mathbf{k})] [k'_j F_i(\mathbf{k}') + k'_i F_j(\mathbf{k}')] }{4} e^{i(\mathbf{k}+\mathbf{k}')\cdot\mathbf{R}} u_{\mathbf{k}} u_{\mathbf{k}'} d^3\mathbf{R} \\ &= \frac{(\lambda + \mu)}{2L} \sum_{\mathbf{k}} [\mathbf{k} \cdot \mathbf{F}(\mathbf{k})]^2 u_{\mathbf{k}} u_{-\mathbf{k}} + \frac{\mu}{2L} \sum_{\mathbf{k}} k^2 |F(\mathbf{k})|^2 u_{\mathbf{k}} u_{-\mathbf{k}} \end{aligned} \quad (\text{II.3})$$

Hence the total classical Hamiltonian can be written as Eq. (5) in the main text.

Now for the algebra defined in Eq. (9) in the main text, there is a relevant 2D version

$$\text{sgn}(\mathbf{s}) = \begin{cases} +1, & \text{if } k_x > 0 \\ -1, & \text{if } k_x < 0 \\ \text{sgn}(k_y), & \text{if } k_x = 0 \end{cases}, \quad \text{sgn}(k_y) = \begin{cases} 1, & \text{if } k_y > 0 \\ -1, & \text{if } k_y < 0 \\ 0, & \text{if } k_y = 0 \end{cases} \quad (\text{II.4})$$

The vector sgn function satisfies a few properties which will prove later to be handy:

Lemma 1. $\text{sgn}(-\mathbf{k}) = -\text{sgn}(\mathbf{k})$, for $\forall \mathbf{k}$; $\text{sgn}(\mathbf{k}) = 0$ iff $\mathbf{k} = 0$
 $\text{sgn}(-\mathbf{s}) = -\text{sgn}(\mathbf{s})$, for $\forall \mathbf{s}$; $\text{sgn}(\mathbf{s}) = 0$ iff $\mathbf{s} = 0$.

where “iff” means “if and only if”. The proof is straightforward.

Lemma 2. $\{\text{sgn } \mathbf{s} \geq 0 | \kappa = 0\} \subset \{\text{sgn } \mathbf{k} \geq 0\}$.

Where “ $\{ \}$ ” is the notation for set. “ $X|C$ ” means set X satisfies condition C .

Proof: $\{\text{sgn } \mathbf{s} \geq 0 | \kappa = 0\} = \left\{ \begin{array}{l} k_x > 0, \forall k_y, \kappa = 0 \\ k_x = 0, k_y > 0, \kappa = 0 \\ k_x = 0, k_y = 0, \kappa = 0 \end{array} \right\} \subset \left\{ \begin{array}{l} k_x > 0, \forall k_y, \forall \kappa \\ k_x = 0, k_y > 0, \forall \kappa \\ k_x = 0, k_y = 0, \kappa \geq 0 \end{array} \right\} = \{\text{sgn } \mathbf{k} \geq 0\}$

Lemma 3. $\{\text{sgn } \mathbf{s} \geq 0 | \kappa = 0\} = \{\text{sgn } \mathbf{k} \geq 0 | \kappa = 0\}$

Proof: Using Lemma 2, $\{\text{sgn } \mathbf{s} \geq 0 | \kappa = 0\} = \left\{ \begin{array}{l} k_x > 0, \forall k_y, \kappa = 0 \\ k_x = 0, k_y > 0, \kappa = 0 \\ k_x = 0, k_y = 0, \kappa = 0 \end{array} \right\} = \{\text{sgn } \mathbf{k} \geq 0 | \kappa = 0\}$.

Now the classical Hamiltonian Eq. (6) in the main text can be simplified with Eqs. (7) and (8) as

$$\begin{aligned} H &= \sum_{\mathbf{k}} \frac{\hbar \Omega(\mathbf{k})}{4} (a_{\mathbf{k}}^+ a_{\mathbf{k}} + a_{-\mathbf{k}}^+ a_{-\mathbf{k}} + a_{-\mathbf{k}}^+ a_{-\mathbf{k}} + a_{\mathbf{k}}^+ a_{\mathbf{k}}) \\ &= \sum_{\mathbf{k}} \hbar \Omega(\mathbf{k}) a_{\mathbf{k}}^+ a_{\mathbf{k}} = \sum_{\mathbf{k} \geq 0} \hbar \Omega(\mathbf{k}) a_{\mathbf{k}}^+ a_{\mathbf{k}} + \sum_{\mathbf{k} < 0} \hbar \Omega(\mathbf{k}) b_{-\mathbf{k}}^+ b_{-\mathbf{k}} \\ &= \sum_{\mathbf{k} \geq 0} \hbar \Omega(\mathbf{k}) \left(a_{\mathbf{k}}^+ a_{\mathbf{k}} + \frac{1}{2} \right) + \sum_{\mathbf{k} \geq 0} \hbar \Omega(\mathbf{k}) \left(b_{\mathbf{k}}^+ b_{\mathbf{k}} + \frac{1}{2} \right) \end{aligned} \quad (\text{II.5})$$

where we have used the fact that $\Omega(\mathbf{k} = \mathbf{0}) = 0$, and we use the short-hand notation $\sum_{\mathbf{k} \geq 0}$ standing for summing over \mathbf{k} for all $\text{sgn } \mathbf{k} \geq 0$.

III. Derivation of electron-dislocation interaction Hamiltonian

For electron-dislocation scattering, with the generic interaction Hamiltonian between electron and ions in Eq. (12) of main text, we have

$$\begin{aligned} \sum_{j=1}^N \nabla_{\mathbf{R}} V_{ei}(\mathbf{R} - \mathbf{R}_j^0) \cdot \mathbf{u}_j &= \frac{N}{VA} \sum_{\substack{\mathbf{q} \in \text{IBZ}, \mathbf{G} \\ \mathbf{k} = (\mathbf{s}, \kappa)}} V_{\mathbf{q}+\mathbf{G}} e^{i(\mathbf{q}+\mathbf{G}) \cdot \mathbf{R}} [i(\mathbf{q} + \mathbf{G}) \cdot \mathbf{F}(\mathbf{k})] \sqrt{\frac{\hbar}{2m_{\mathbf{k}} \Omega_{\mathbf{k}}}} (a_{\mathbf{k}} + a_{-\mathbf{k}}^+) \delta_{\mathbf{k}, \mathbf{q}+\mathbf{G}} \\ &= \frac{N}{VA} \sum_{\mathbf{k}} V_{\mathbf{k}} e^{i\mathbf{k} \cdot \mathbf{R}} [i\mathbf{k} \cdot \mathbf{F}(\mathbf{k})] \sqrt{\frac{\hbar}{2m_{\mathbf{k}} \Omega_{\mathbf{k}}}} (a_{\mathbf{k}} + a_{-\mathbf{k}}^+) \end{aligned}$$

Thus the interacting Hamiltonian Eq. (12) in the main text can now be simplified as

$$\begin{aligned}
H_{e-dis} &= \int d^3\mathbf{R} \rho_e(\mathbf{R}) \sum_{j=1}^N \nabla_{\mathbf{R}} V_{ei}(\mathbf{R} - \mathbf{R}_j^0) \cdot \mathbf{u}_j \\
&= \int d^3\mathbf{R} \frac{e}{V} \sum_{\mathbf{k}\mathbf{p}\sigma} e^{-i\mathbf{p}\cdot\mathbf{R}} c_{\mathbf{k}'+\mathbf{p}\sigma}^\dagger c_{\mathbf{k}'\sigma} \frac{N}{VA} \sum_{\mathbf{k}} V_{\mathbf{k}} e^{i\mathbf{k}\cdot\mathbf{R}} [\mathbf{k} \cdot \mathbf{F}(\mathbf{k})] \sqrt{\frac{\hbar}{2m_{\mathbf{k}}\Omega_{\mathbf{k}}}} (a_{\mathbf{k}} + a_{-\mathbf{k}}^\dagger) \\
&= \frac{eN}{VA} \sum_{\mathbf{k}'\sigma} c_{\mathbf{k}'+\mathbf{k}\sigma}^\dagger c_{\mathbf{k}'\sigma} \sum_{\mathbf{k}} V_{\mathbf{k}} [\mathbf{k} \cdot \mathbf{F}(\mathbf{k})] \sqrt{\frac{\hbar}{2m_{\mathbf{k}}\Omega_{\mathbf{k}}}} (a_{\mathbf{k}} + a_{-\mathbf{k}}^\dagger) \equiv \sum_{\mathbf{k}\mathbf{k}'\sigma} g_{\mathbf{k}} c_{\mathbf{k}'+\mathbf{k}\sigma}^\dagger c_{\mathbf{k}'\sigma} (a_{\mathbf{k}} + a_{-\mathbf{k}}^\dagger)
\end{aligned}$$

IV. Effective electron action using functional integral approach

To simplify the effective action Eq. (22) in the main text, Fourier transform is first performed,

$$\begin{aligned}
e^{-S_{eff}[\bar{\psi}, \psi]} &\equiv e^{-S_e[\bar{\psi}, \psi]} \int D[\bar{d}, d] \prod_{ns} \int \frac{d\bar{k}_{ns}}{2\pi} \frac{dk_{ns}}{2\pi} e^{i\bar{k}_{ns}(d_{ns0} - C_s)} e^{ik_{ns}(\bar{d}_{ns0} - C_s)} e^{-S_{dis}[\bar{d}, d] - S_{e-dis}[\bar{\psi}, \psi, \bar{d}, d]} \\
&= e^{-S_e[\bar{\psi}, \psi]} \times \int D[\bar{d}, d] D[\bar{k}, k] e^{i \sum_{n,s \geq 0} (\bar{k}_{ns} d_{ns0} + k_{ns} \bar{d}_{ns0} - C_s k_{ns} - C_s \bar{k}_{ns})} e^{-S_{dis}[\bar{d}, d] - S_{e-dis}[\bar{\psi}, \psi, \bar{d}, d]}
\end{aligned} \tag{IV.1}$$

Where we have defined that functional measure $D[\bar{k}, k] \equiv \prod_{ns} \int \frac{d\bar{k}_{ns}}{2\pi} \frac{dk_{ns}}{2\pi}$.

Further integrating over dislon degree of freedom, and using Lemma 3, we have

$$\begin{aligned}
e^{-S_{eff}[\bar{\psi}, \psi]} &= e^{-S_e[\bar{\psi}, \psi]} \int D[\bar{d}, d] D[\bar{k}, k] \times \exp \left[\sum_{ns \geq 0} -iC_s (\bar{k}_{ns} + k_{ns}) \right] \times \\
&\exp \left[- \sum_{nk \geq 0} \bar{d}_{kn} (-i\omega_n + \hbar\Omega_{\mathbf{k}}) d_{kn} + \sum_{nk \geq 0} \left(i\bar{k}_{ns} \delta_{\kappa 0} - \frac{g_{\mathbf{k}}}{\sqrt{\beta/2}} \rho_{nk} \right) d_{nk} + \sum_{nk \geq 0} \left(ik_{ns} \delta_{\kappa 0} - \frac{g_{\mathbf{k}}^*}{\sqrt{\beta/2}} \rho_{-n-\mathbf{k}} \right) \bar{d}_{nk} \right] \\
&= e^{-S_e[\bar{\psi}, \psi]} \times \exp \left[\sum_{nk \geq 0} \frac{2g_{\mathbf{k}}^* g_{\mathbf{k}}}{\beta(-i\omega_n + \hbar\Omega_{\mathbf{k}})} \rho_{-n-\mathbf{k}} \rho_{nk} \right] \times \int D[\bar{k}, k] \times \\
&\exp \left[\sum_{ns \geq 0} - \frac{\bar{k}_{ns} k_{ns}}{(-i\omega_n + \hbar\Omega_{\mathbf{s}})} - i \left(\frac{g_{\mathbf{s}}^* \rho_{-n-\mathbf{s}}}{\sqrt{\beta/2}(-i\omega_n + \hbar\Omega_{\mathbf{s}})} + C_s \right) \bar{k}_{ns} - i \left(\frac{g_{\mathbf{s}} \rho_{ns}}{\sqrt{\beta/2}(-i\omega_n + \hbar\Omega_{\mathbf{s}})} + C_s \right) k_{ns} \right]
\end{aligned}$$

Now we further integrate over the $[\bar{k}, k]$ fields,

$$e^{-S_{eff}[\bar{\psi}, \psi]} = e^{-S_e[\bar{\psi}, \psi]} \times \exp \left[\sum_{n\mathbf{k} \geq 0} \frac{2g_{\mathbf{k}}^* g_{\mathbf{k}}}{\beta(-i\omega_n + \hbar\Omega_{\mathbf{k}})} \rho_{-n-\mathbf{k}} \rho_{n\mathbf{k}} \right] \times$$

$$\exp \left[\sum_{ns \geq 0} \left(-\frac{2g_s^* g_s \rho_{-n-s} \rho_{ns}}{\beta(-i\omega_n + \hbar\Omega_s)} - \frac{C_s g_s}{\sqrt{\beta/2}} \rho_{ns} - \frac{g_s^* C_s}{\sqrt{\beta/2}} \rho_{-n-s} - C_s^2(-i\omega_n + \hbar\Omega_s) \right) \right]$$

Where the constant terms $C_s^2(-i\omega_n + \hbar\Omega_s)$ can be neglected. Now we deal with the quartic term $\rho_{-n-\mathbf{k}} \rho_{n\mathbf{k}}$. Using Lemma 3, we have $\sum_{\mathbf{k} \geq 0} \dots - \sum_{s \geq 0} \delta_{\kappa 0} \dots = \sum_{\mathbf{k} \geq 0} \dots - \sum_{\mathbf{k} \geq 0} \delta_{\kappa 0} \dots = \sum_{\mathbf{k} \geq 0 | \kappa \neq 0} \dots = \frac{1}{2} \sum_{\mathbf{k} | \kappa \neq 0} \dots$, and using Lemma 1, and the fact $g_{-s} = g_s^*$, $\sum_n = \sum_{-n}$

we have the effective action can further be reduced as

$$e^{-S_{eff}[\bar{\psi}, \psi]} = e^{-S_e[\bar{\psi}, \psi]} \times \exp \left[\sum_{n\mathbf{k} | \kappa \neq 0} \frac{g_{\mathbf{k}}^* g_{\mathbf{k}}}{\beta(-i\omega_n + \hbar\Omega_{\mathbf{k}})} \rho_{-n-\mathbf{k}} \rho_{n\mathbf{k}} \right] \times \exp \left[-\sum_{ns} \left(\frac{C_s g_s}{\sqrt{2\beta}} \rho_{ns} + \frac{g_s^* C_s}{\sqrt{2\beta}} \rho_{-n-s} \right) \right]$$

$$= e^{-S_e[\bar{\psi}, \psi]} \times \exp \left[\sum_{n\mathbf{k} | \kappa \neq 0} \frac{\hbar\Omega_{\mathbf{k}} g_{\mathbf{k}}^* g_{\mathbf{k}}}{\beta(\omega_n^2 + \hbar^2 \Omega_{\mathbf{k}}^2)} \rho_{-n-\mathbf{k}} \rho_{n\mathbf{k}} - \sum_{\mathbf{k} n \sigma} \sum_{ms} \frac{C_s}{\sqrt{2\beta}} (\bar{\psi}_{n+m, \mathbf{k}+\mathbf{s}\sigma} g_s + \bar{\psi}_{n-m, \mathbf{k}-\mathbf{s}\sigma} g_s^*) \psi_{n\mathbf{k}\sigma} \right]$$

Finally, we have the effective action can be written as

$$S_{eff}[\bar{\psi}, \psi] = S_e[\bar{\psi}, \psi] - \sum_{n\mathbf{k} | \kappa \neq 0} \frac{\hbar\Omega_{\mathbf{k}} g_{\mathbf{k}}^* g_{\mathbf{k}}}{\beta(\omega_n^2 + \hbar^2 \Omega_{\mathbf{k}}^2)} \rho_{-n-\mathbf{k}} \rho_{n\mathbf{k}} + \sum_{ns} \left(\frac{C_s g_s}{\sqrt{2\beta}} \rho_{ns} + \frac{g_s^* C_s}{\sqrt{2\beta}} \rho_{-n-s} \right) \quad (\text{IV.2})$$

This is equivalent with Eq. (23) in the main text by noticing that $\rho_{ns} \equiv \sum_{\mathbf{k}' m \sigma} \bar{\psi}_{m+n, \mathbf{k}'+\mathbf{s}\sigma} \psi_{m\mathbf{k}'\sigma}$ where \mathbf{s} is the in-plane 2D momentum.

V. Electron-classical dislocation interaction

For an edge dislocation, $\mathbf{b} = (b \ 0 \ 0)$, $\mathbf{b} \cdot \mathbf{s} = bk_x$, $\mathbf{n} \cdot \mathbf{s} = s \sin \theta$ and hence we have the magnitude of the classical scattering amplitude based on Eq. (25) in the main text as

$$A_s^{Edge} = \frac{N}{2VL} eV_s \left(\frac{1-2\nu}{1-\nu} \right) \frac{b \sin \theta}{\sqrt{k_x^2 + k_y^2}} \quad (\text{V.1})$$

where θ is the angle between Burgers vector and dislocation line direction. Now performing Fourier transform, Assuming V_s is independent of \mathbf{s} due to screening effect, we have (Assuming $\mathbf{r} \neq 0$)

$$\begin{aligned}
A^{Edge}(\mathbf{r}) &= \int A_s^{Edge} e^{i\mathbf{s} \cdot \mathbf{r}} \frac{d^2 \mathbf{s}}{4\pi^2} = \frac{N}{2VL} \frac{4\pi Ze^2}{k_{TF}^2} \sin \theta \left(\frac{1-2\nu}{1-\nu} \right) \frac{b}{4\pi^2} \int_{-\infty}^{+\infty} dk_y e^{ik_y y} \int_{-\infty}^{+\infty} dk_x \frac{e^{ik_x x}}{\sqrt{k_x^2 + k_y^2}} \\
&= \frac{N}{2VL} \sqrt{n_{dis}} \frac{4\pi Ze^2}{k_{TF}^2} \sin \theta \left(\frac{1-2\nu}{1-\nu} \right) \frac{b}{4\pi^2} \underbrace{\int_{-\infty}^{+\infty} dk_y 2K_0(|xk_y|) e^{ik_y y}}_{\text{}} \\
&= \frac{N}{2VL} \sqrt{n_{dis}} \frac{4\pi Ze^2}{k_{TF}^2} \times \frac{b \sin \theta}{4\pi^2} \left(\frac{1-2\nu}{1-\nu} \right) \underbrace{\frac{2\pi}{\sqrt{x^2 + y^2}}}_{\text{}} = \frac{N \sqrt{n_{dis}}}{VL} \frac{2\pi Ze^2}{k_{TF}^2} \times \frac{b}{2\pi} \left(\frac{1-2\nu}{1-\nu} \right) \frac{\sin \theta}{r} \\
&\propto \frac{b}{2\pi} \left(\frac{1-2\nu}{1-\nu} \right) \frac{\sin \theta}{r}
\end{aligned} \tag{V.2}$$

which shows excellent agreement with the well-known classical electron-dislocation scattering.

For the elastic scattering rate, we have

$$\begin{aligned}
\Gamma_{\mathbf{k}} &= \frac{\pi}{2} \sum_{\mathbf{s}} \left| \langle \mathbf{k} + \mathbf{s} | \hat{A}_c | \mathbf{k} \rangle \right|^2 \delta(\varepsilon_{\mathbf{k}+\mathbf{s}} - \varepsilon_{\mathbf{k}}) = \frac{\pi}{\hbar} \sum_{\mathbf{s}} |A_s|^2 \delta(\varepsilon_{\mathbf{k}+\mathbf{s}} - \varepsilon_{\mathbf{k}}) = \frac{L^2}{4\pi\hbar} \int |A_s|^2 \delta(\varepsilon_{\mathbf{k}+\mathbf{s}} - \varepsilon_{\mathbf{k}}) d^2 \mathbf{s} \\
&= \frac{1}{8\pi} \left(\frac{eN}{2V} \right)^2 n_{dis} b^2 \left(\frac{1-2\nu}{1-\nu} \right)^2 \int d\theta_s \int_0^{k_F} |V_s|^2 \sin^2 \theta_s \delta(\varepsilon_{\mathbf{k}+\mathbf{s}} - \varepsilon_{\mathbf{k}}) \frac{ds}{s} \\
&= \frac{1}{8\pi} \left(\frac{eN}{2V} \right)^2 n_{dis} b^2 \left(\frac{1-2\nu}{1-\nu} \right)^2 \int d\theta_s \int_0^{k_F} \frac{(4\pi Ze)^2}{(s^2 + k_{TF}^2)^2} \sin^2 \theta_s \frac{m^*}{\hbar^2 k} \delta(s + 2k \cos \theta_{ks}) \frac{ds}{s} \\
&= -\frac{\pi m^*}{4\hbar^2 k^2} \left(\frac{Ze^2 N}{V} \right)^2 n_{dis} b^2 \left(\frac{1-2\nu}{1-\nu} \right)^2 \int_0^{2\pi} \frac{\sin^2 \theta_s}{(4k^2 \cos^2 \theta_{ks} + k_{TF}^2)^2 \cos \theta_{ks}} d\theta_s
\end{aligned} \tag{V.3}$$

where θ_s is the angle of \mathbf{s} with \mathbf{x} axis, and θ_{ks} is the angle between \mathbf{k} and \mathbf{s} , and the energy conservation can be written as $\delta(\varepsilon_{\mathbf{k}+\mathbf{s}} - \varepsilon_{\mathbf{k}}) = \frac{m^*}{\hbar^2 k} \delta(s + 2k \cos \theta_{ks})$. Now if we assume a long wavelength limit $k \ll k_{TF}$ and neglected the complex angle-dependent integration which is of order of magnitude $\sim O(1)$, the relaxation rate can finally be written as Eq. (29) in the main text.

VI. Electron- quantum dislocation interaction: superconductivity

From Eq. (31) in the main text, performing Fourier transform of operator $c_{\mathbf{k}}^+ = \frac{1}{\sqrt{V}} \int d^3\mathbf{r} e^{i\mathbf{k}\cdot\mathbf{r}} c^+(\mathbf{r})$,

we have

$$\begin{aligned} & \sum_{\mathbf{q}\mathbf{k}\mathbf{k}'} c_{\mathbf{k}+\mathbf{q}\uparrow}^+ c_{-\mathbf{k}\downarrow}^+ c_{-\mathbf{k}'+\mathbf{q}\downarrow} c_{\mathbf{k}'\uparrow} = \frac{1}{V^2} \int d^3\mathbf{r} d^3\mathbf{r}_1 d^3\mathbf{r}_2 d^3\mathbf{r}_3 c_{\uparrow}^+(\mathbf{r}) c_{\downarrow}^+(\mathbf{r}_1) c_{\downarrow}^+(\mathbf{r}_2) c_{\uparrow}^+(\mathbf{r}_3) \sum_{\mathbf{k}} e^{i\mathbf{k}\cdot(\mathbf{r}-\mathbf{r}_1)} \sum_{\mathbf{q}} e^{i\mathbf{q}\cdot(\mathbf{r}-\mathbf{r}_2)} \sum_{\mathbf{k}'} e^{i\mathbf{k}'\cdot(\mathbf{r}_2-\mathbf{r}_3)} \\ &= \frac{1}{V^2} \int d^3\mathbf{r} d^3\mathbf{r}_1 d^3\mathbf{r}_2 d^3\mathbf{r}_3 c_{\uparrow}^+(\mathbf{r}) c_{\downarrow}^+(\mathbf{r}_1) c_{\downarrow}^+(\mathbf{r}_2) c_{\uparrow}^+(\mathbf{r}_3) V \delta(\mathbf{r}-\mathbf{r}_1) V \delta(\mathbf{r}-\mathbf{r}_2) V \delta(\mathbf{r}_2-\mathbf{r}_3) \\ &= V \int d^3\mathbf{r} c_{\uparrow}^+(\mathbf{r}) c_{\downarrow}^+(\mathbf{r}) c_{\downarrow}^+(\mathbf{r}) c_{\uparrow}^+(\mathbf{r}) \end{aligned}$$

which recovers the Eq. (33) in the main text.

Quantitatively, to obtain the superconducting transition temperature with the presence of dislocations, we adopt the auxiliary field method by doing the Hubbard-Stratonovich transformation,

$$\begin{aligned} Z &= \int D[\bar{\psi}, \psi] \exp \left[- \sum_{\mathbf{k}n} \bar{\psi}_{n\mathbf{k}\uparrow} (-ip_n + E_{\mathbf{k}} - \mu' + i\Gamma_{\mathbf{k}}) \psi_{n\mathbf{k}\uparrow} - \sum_{\mathbf{k}n} \bar{\psi}_{n\mathbf{k}\downarrow} (-ip_n + E_{\mathbf{k}} - \mu' - i\Gamma_{\mathbf{k}}) \psi_{n\mathbf{k}\downarrow} \right] \\ &\times \exp \left(+ g_T \int_0^\beta d\tau \int d^3\mathbf{r} \bar{\psi}_{\uparrow}(\mathbf{r}) \bar{\psi}_{\downarrow}(\mathbf{r}) \psi_{\downarrow}(\mathbf{r}) \psi_{\uparrow}(\mathbf{r}) \right) \\ &= \int D[\bar{\psi}, \psi] \exp \left[- \sum_{\mathbf{k}n} \bar{\psi}_{n\mathbf{k}\uparrow} (-ip_n + E_{\mathbf{k}} - \mu' + i\Gamma_{\mathbf{k}}) \psi_{n\mathbf{k}\uparrow} - \sum_{\mathbf{k}n} \bar{\psi}_{n\mathbf{k}\downarrow} (-ip_n + E_{\mathbf{k}} - \mu' - i\Gamma_{\mathbf{k}}) \psi_{n\mathbf{k}\downarrow} \right] \\ &\times \int D[\bar{\Delta}, \Delta] \exp \left[- \frac{1}{g_T} \int_0^\beta d\tau \int d^3\mathbf{r} \bar{\Delta}(\mathbf{r}) \Delta(\mathbf{r}) + \int_0^\beta d\tau \int d^3\mathbf{r} \bar{\Delta}(\mathbf{r}) \psi_{\downarrow}(\mathbf{r}) \psi_{\uparrow}(\mathbf{r}) + \int_0^\beta d\tau \int d^3\mathbf{r} \bar{\Delta}(\mathbf{r}) \psi_{\downarrow}(\mathbf{r}) \psi_{\uparrow}(\mathbf{r}) \right] \\ &= \int D[\bar{\Delta}, \Delta] \exp \left[- \frac{1}{g_T} \int_0^\beta d\tau \int d^3\mathbf{r} \bar{\Delta}(\mathbf{r}) \Delta(\mathbf{r}) \right] \times \\ &D[\bar{\psi}, \psi] \exp \left[- \int_0^\beta d\tau \int d^3\mathbf{r} \begin{pmatrix} \bar{\psi}_{\uparrow} & \bar{\psi}_{\downarrow} \end{pmatrix} \begin{pmatrix} \partial_\tau + E - \mu' + i\Gamma & \Delta \\ \bar{\Delta} & \partial_\tau - E + \mu' + i\Gamma \end{pmatrix} \begin{pmatrix} \psi_{\uparrow} \\ \psi_{\downarrow} \end{pmatrix} \right] \end{aligned}$$

The effective action can now be written as

$$S[\bar{\Delta}, \Delta] = \frac{1}{g_T} \int_0^\beta d\tau \int d^3\mathbf{r} \bar{\Delta}(\mathbf{r}) \Delta(\mathbf{r}) - \text{Tr} \ln \beta \begin{bmatrix} \partial_\tau + E - \mu' + i\Gamma & \Delta \\ \bar{\Delta} & \partial_\tau - E + \mu' + i\Gamma \end{bmatrix} \quad (\text{VI.1})$$

On the mean-field level, assuming a spatial-independent Δ field $\Delta(\mathbf{r}) \equiv \Delta$, we have

$$\begin{aligned} \frac{\delta S[\bar{\Delta}, \Delta]}{\delta \Delta} = 0 &\Rightarrow \frac{1}{g_T} \bar{\Delta} = \frac{1}{\beta V} \sum_{n\mathbf{k}} \begin{pmatrix} -ip_n + E_{\mathbf{k}} - \mu' + i\Gamma_{\mathbf{k}} & \Delta \\ \bar{\Delta} & -ip_n - E_{\mathbf{k}} + \mu' + i\Gamma_{\mathbf{k}} \end{pmatrix}^{-1} \begin{pmatrix} 0 & 1 \\ 0 & 0 \end{pmatrix} \\ \frac{1}{g_T} \bar{\Delta} &= -\frac{1}{\beta V} \sum_{n\mathbf{k}} \frac{-\bar{\Delta}}{(E_{\mathbf{k}} - \mu')^2 + (p_n - \Gamma_{\mathbf{k}})^2 + |\Delta|^2} \Rightarrow \frac{1}{g_T} = \frac{1}{\beta V} \sum_{n\mathbf{k}} \frac{1}{(E_{\mathbf{k}} - \mu')^2 + (p_n - \Gamma_{\mathbf{k}})^2 + |\Delta|^2} \end{aligned} \quad (\text{VI.2})$$

To compute the frequency summation in Eq. (VI.2), we use complex integration method. Defining an contour integral in the complex plane $I = -\frac{1}{2\pi i} \oint dz \frac{n_F(z)}{(z - i\Gamma_{\mathbf{k}})^2 - (E_{\mathbf{k}} - \mu')^2 - |\Delta|^2}$, where n_F is

the Fermi occupation function. The integrand has poles at $z = ip_n$ and $z = i\Gamma_{\mathbf{k}} \pm \sqrt{\varepsilon_{\mathbf{k}}^2 + |\Delta|^2}$ in the entire complex plane. Now using the residue theorem and using the contour integral over the whole plane, we have

$$I = 0 = -\sum_n \frac{1}{(ip_n - i\Gamma_{\mathbf{k}})^2 - (E_{\mathbf{k}} - \mu')^2 - |\Delta|^2} \times \left(-\frac{1}{\beta} \right) - \frac{n_F(i\Gamma_{\mathbf{k}} + \sqrt{(E_{\mathbf{k}} - \mu')^2 + |\Delta|^2})}{2\sqrt{(E_{\mathbf{k}} - \mu')^2 + |\Delta|^2}} + \frac{n_F(i\Gamma_{\mathbf{k}} - \sqrt{(E_{\mathbf{k}} - \mu')^2 + |\Delta|^2})}{2\sqrt{(E_{\mathbf{k}} - \mu')^2 + |\Delta|^2}}$$

Substituting back to Eq. (VI.2), we have

$$\frac{1}{g_T} = \frac{1}{V} \sum_{\mathbf{k}} \frac{n_F(i\Gamma_{\mathbf{k}} - \lambda_{\mathbf{k}})}{2\lambda_{\mathbf{k}}} - \frac{n_F(i\Gamma_{\mathbf{k}} + \lambda_{\mathbf{k}})}{2\lambda_{\mathbf{k}}} \quad (\text{VI.3})$$

Where we have defined the quasiparticle excitation energy $\lambda_{\mathbf{k}} = \sqrt{(E_{\mathbf{k}} - \mu')^2 + |\Delta|^2} > 0$. Further computing ($\lambda(\xi) = \sqrt{(\xi - \mu')^2 + |\Delta|^2} > 0$), we have

$$\begin{aligned} \frac{1}{g_T} &= \frac{1}{g_{ph} + g_{dis}} = \frac{1}{V} \sum_{\mathbf{k}} \frac{1}{2\sqrt{\lambda_{\mathbf{k}}^2 + \Gamma_{\mathbf{k}}^2}} [n_F(i\Gamma_{\mathbf{k}} - \lambda_{\mathbf{k}}) - n_F(i\Gamma_{\mathbf{k}} + \lambda_{\mathbf{k}})] \\ &= N(\mu) \int_0^{\omega_D} \frac{n_F(i\Gamma - \lambda(\xi)) - n_F(i\Gamma + \lambda(\xi))}{\lambda(\xi)} d\xi \\ &= N(\mu') \int_0^{\omega_D} \frac{\tanh\left(\frac{\lambda(\xi) + i\Gamma}{2T}\right) + \tanh\left(\frac{\lambda(\xi) - i\Gamma}{2T}\right)}{2\lambda(\xi)} d\xi \end{aligned} \quad (\text{VI.4})$$

where we have defined the density of states at the Fermi level as $N(\mu')$. Written in this way, Eq. (VI.4) resembles very much the original BCS gap equation,

$$\frac{1}{g_{ph}} = N(\mu) \int_0^{\omega_D} \frac{\tanh\left(\frac{\lambda(\xi)}{2T}\right)}{\lambda(\xi)} d\xi \quad (\text{VI.5})$$

The meaning of $N(\mu)$ means it is taken from the bare electron spectra $\varepsilon_{\mathbf{k}}$ prior to renormalization, with a different density of states. Noticing that at $T=T_c$, the superconducting energy gap $|\Delta|=0$, we obtain the corresponding T_c equation which is the Eq. (34) in the main text.

VII. Dimensions of all relevant parameters

$$\begin{aligned} [H] &= [T] = [U] = M^{+1}L^2T^{-2}, \quad [F(\mathbf{k})] = L^3, \quad [\mathbf{u}_i(\mathbf{R})] = L, \quad [\mathbf{u}_{\mathbf{k}}] = 1, \quad [\lambda] = [\mu] = M^{+1}L^{-1}T^{-2}, \\ [\rho] &= M^{+1}L^{-3}, \quad [T(\mathbf{k})] = M^{+1}L^3, \quad [U(\mathbf{k})] = M^{+1}L^3T^{-2}, \quad [m_{\mathbf{k}}] = M^{+1}L^2, \quad [\Omega_{\mathbf{k}}] = T^{-1}, \quad [\hbar] = M^{+1}L^{+2}T^{-1}, \\ [Z_{\mathbf{k}}] &\equiv 1, \quad [e] = M^{1/2}L^{3/2}T^{-1} \quad (\text{static Coulomb}), \quad [V_{\mathbf{q}}] = M^{+1/2}L^{+7/2}T^{-1}, \quad [eV_{\mathbf{q}}] = M^{+1}L^{+5}T^{-2}, \\ [\rho_e(\mathbf{r})] &= M^{1/2}L^{-3/2}T^{-1}, \quad [c(\mathbf{r})] = L^{-3/2}, \quad [g_T] = [g_{ph}] = [g_{dis}] = M^{+1}L^5T^{-2}, \quad [\Delta(\mathbf{r})] = M^{+1}L^2T^{-2} = [H], \\ [\psi_{np}] &= [\chi_{np}] = [d_{np}] = [C_s] = M^{-1/2}L^{-1}T^{+1} = [H^{-1/2}], \quad [\beta] = [\rho_{nk}] = M^{-1}L^{-2}T^{+2} = [H^{-1}], \\ [g_{\mathbf{k}}] &= M^{+1}L^2T^{-2} = [H], \quad [T_c] = M^{+1}L^2T^{-2} = [H], \quad [N(E_F)] = M^{-1}L^{-5}T^{+2} = [g_{ph}]^{-1}. \end{aligned}$$

However, the experimental magnitude of g_{ph} is usually given in energy units, hence to make the quantum-to-classical ratio comparable, we express all the magnitudes in the unit of energy as: $[g_{dis}] = [g_{ph}] = [\Gamma] = [\omega_D] = M^{+1}L^2T^{-2}$ by dividing both the numerator and denominator by the volume V .

References

1. Hirth JP, Lothe J. *Theory of dislocations*, 2nd edn. Krieger Pub. Co.: Malabar, FL, 1992.